Check for updates

Modulating tumor mechanics with nanomedicine for cancer therapy

Qingfu Zhao,†[a] Jitang Chen, [ID] †[a] Zhijie Zhang,[a] Chen Xiao,[a] Haowen Zeng,[a] Chen Xu,[a] Xiangliang Yang [ID] [a,b,c,d,e] and Zifu Li [ID] *[a,b,c,d,e]

Over the past several decades, the importance of the tumor mechanical microenvironment (TMME) in cancer progression or cancer therapy has been recognized by researchers worldwide. The abnormal mechanical properties of tumor tissues include high mechanical stiffness, high solid stress, and high interstitial fluid pressure (IFP), which form physical barriers resulting in suboptimal treatment efficacy and resistance to different types of therapy by preventing drugs infiltrating the tumor parenchyma. Therefore, preventing or reversing the establishment of the abnormal TMME is critical for cancer therapy. Nanomedicines can enhance drug delivery by exploiting the enhanced permeability and retention (EPR) effect, so nanomedicines that target and modulate the TMME can further boost antitumor efficacy. Herein, we mainly discuss the nanomedicines that can regulate mechanical stiffness, solid stress, and IFP, with a focus on how nanomedicines change abnormal mechanical properties and facilitate drug delivery. We first introduce the formation, characterizing methods and biological effects of tumor mechanical properties. Conventional TMME modulation strategies will be briefly summarized. Then, we highlight representative nanomedicines capable of modulating the TMME for augmented cancer therapy. Finally, current challenges and future opportunities for regulating the TMME with nanomedicines will be provided.

Introduction

An abnormal mechanical microenvironment (stiffening) is a significant common feature of many solid tumors,[1] such as breast cancer, liver cancer, pancreatic cancer, and brain cancer, to name a few, while raised stiffness has become the theoretical basis for clinical palpation of solid malignancies. Compared with normal breast tissue, the stiffness of breast cancer tissue increases by nearly 19-fold.[2] Likewise, the average stiffness of healthy liver is 5 kPa, whereas the stiffness of advanced hepatocellular carcinoma exceeds 20 kPa.[3] The

[a]*National Engineering Research Center for Nanomedicine, College of Life Science and Technology, Huazhong University of Science and Technology, Wuhan, 430074, P. R. China. E-mail: zifuli@hust.edu.cn*
[b]*Key Laboratory of Molecular Biophysics of Ministry of Education, College of Life Science and Technology, Huazhong University of Science and Technology, Wuhan, 430074, P. R. China*
[c]*Hubei Key Laboratory of Bioinorganic Chemistry and Materia Medical, Huazhong University of Science and Technology, Wuhan, 430074, P. R. China*
[d]*Hubei Engineering Research Center for Biomaterials and Medical Protective Materials, Huazhong University of Science and Technology, Wuhan, 430074, P. R. China*
[e]*Hubei Bioinformatics and Molecular Imaging Key Laboratory, College of Life Science and Technology, Huazhong University of Science and Technology, Wuhan, 430074, P. R. China*
†These authors contributed equally.

average stiffness of normal pancreatic tissue is approximately 2.5 kPa, while pancreatic cancer tissue exhibits an average stiffness of 6.1 kPa.[4] These clinical observations underline the importance of measuring tissue mechanical properties, especially the tissue stiffness, in distinguishing between healthy and diseased tissues. The extracellular matrix (ECM) composed of a large number of biological macromolecules such as proteins and enzymes accumulated in tumor tissues, the high interstitial fluid pressure (IFP) of tumor tissues caused by the combination of tumor blood vessels with abnormal structure and dysfunction and lymph vessels with high compression and loss of function, as well as the solid stress brought by the rapid proliferation of malignant cells, are the main causes for the stiffening of these tissues.[5] This deteriorated mechanical microenvironment promotes tumor progression through a variety of mechanisms. First, the sclerotic tumor tissue directly regulates the integrin signal pathway of the interaction between tumor cells/stromal cells and ECM through mechanical signals to accelerate the tumor progression.[6] Second, the hardened tumor tissue initiates the process of epithelial–mesenchymal transformation (EMT) and promotes the invasion and metastasis of cancer cells.[7] Third, abundant ECM components, such as collagen and hyaluronic acid (HA), high IFP, and accumulated solid stress of tumor tissues form a physical barrier, preventing the penetration and uniform distribution of chemotherapy drugs (including small

molecular drugs and nanomedicines) and the infiltration of effector T cells into tumor parenchyma.[8] Fourth, the stiffened tumor tissues will further compress the blood vessels and lymphatic vessels in tumor tissues, reduce blood perfusion, cause tumor hypoxia, and ultimately lead to the tumor cells' insensitivity to antitumor drugs, the depletion of effector T cells and the formation of an immunosuppressive microenvironment.[9] Therefore, interrupting tumor mechanics can significantly delay the occurrence, development, invasion and metastasis of tumors, and enhance the delivery efficiency and antitumor effects of chemotherapy, targeted therapy and immunotherapy.[10] Small molecule β-aminopropionitrile (BAPN) slows down the progression of breast cancer by inhibiting the cross-linking of type I collagen protein mediated by lysyl oxidase (LOX) and reducing matrix hardness. However, BAPN failed to enter clinical trial due to safety concerns.[11] Another enzyme that cross-links type I collagen is lysyl oxidase-like 2 (LOXL2). The LOXL2-specific monoclonal antibody AB0023 effectively prevents the cross-linking of type I collagen in breast cancer matrix and delays the development of tumors.[12] Transforming growth factor-β (TGF-β)-neutralizing antibody 1D11 can improve the antitumor efficacy of chemotherapy drugs by reshaping the tumor mechanical microenvironment (TMME) of breast cancers, inhibiting the synthesis of type I collagen.[13] Polyethylene glycol recombinant human hyaluronidase (PEGPH20) improves the TMME by degrading HA of pancreatic cancer, improves the antitumor effect of gemcitabine and prolongs the survival period of mice.[14] Numerous phase II clinical trials have been carried out on PEGPH20 in combination with other drugs to treat pancreatic cancers. The marketed drug Plerixafor reduces the degree of fibrosis in metastatic breast cancers by targeting the CXCR4/CXCL12 signaling pathway, relieves tumor immunosuppression, and enhances the inhibitory effect of immune checkpoint blockers (ICB) on tumor growth and distant metastasis.[15] Losartan, a drug clinically used to treat hypertension, reduces the matrix hardness of pancreatic cancer and ovarian cancer by inhibiting the synthesis of type I collagen and HA, promotes the delivery of chemotherapy drugs and antitumor efficacy, and can enhance the infiltration of effector T cells and tumor-killing effect.[15] Multiple phase II clinical studies have been performed on losartan in combination with other chemotherapy drugs and ICB for treatment of pancreatic cancers. These preclinical and clinical studies corroborate that targeting the TMME is conducive to treatments of solid tumors.

Compared with conventional small-molecular antitumor drugs, nanomedicines have several unique advantages. First, nano drug delivery system (NDDS) can improve the pharmacokinetics of small-molecule drugs with poor water solubility, extend their blood half-life, and increase the concentration of small molecular drugs in tumor sites.[16] Second, by conjugating targeted ligands, polypeptides, proteins and antibodies on the surface of nanocarriers, nanomedicines can accurately target tumor tissues and cancer cells, and then specifically kill malignant cells.[17] Third, nanomedicines can reduce drug concentration in normal tissues and thus decrease toxic and side effects towards normal organs and tissues.[9] Fourth, nanocarriers can simultaneously deliver two or more antitumor drugs with different mechanisms of action and realize controlled release of these drugs and precise synchronization of multiple antitumor actions in both time and space.[18] Therefore, cancer nanomedicines have received tremendous attention in the past few decades, and dozens of nanomedicines have been approved for clinical applications, the most famous of which are liposome doxorubicin (Doxil) and paclitaxel albumin nanoparticles (Abraxane).[16] Although clinical data showed that Doxil significantly reduced the cardiac toxicity and side effects of doxorubicin, Doxil did not improve the overall survival of patients with solid tumors.[19] One of the key reasons is that the abnormal TMME of solid tumors severely impedes tumor accumulation and distribution of Doxil.[20] To that end, several clinical treatments, including radiation therapy,[21–25] hyperbaric oxygen therapy,[26–30] and enzymatic therapy[31–33] have been leveraged to tackle the physical obstacles and augment nanomedicine antitumor efficacy. Furthermore, multifarious nanomedicines capable of inter-

Qingfu Zhao received his BS degree in Chinese Medicine from Shaanxi University of Traditional Chinese Medicine in 2019 and Master's degree in Bioengineering from Fujian Agriculture and Forestry University in 2022. Then he joined Prof. Zifu Li's group to pursue a PhD degree at the College of Life Science and Technology, Huazhong University of Science and Technology. His research focuses on cancer immunotherapy.

Qingfu Zhao

Chen Jitang received his PhD degree from the Huazhong University of Science and Technology in 2022. He worked on developing smart nanomedicines that modulate the aberrant tumor mechanical microenvironment for effective cancer therapy during his PhD, spending time under the supervision of Professor Zifu Li.

Jitang Chen

rupting the TMME by means of photodynamic therapy[34–36] and photothermal therapy[37–46] have been prepared and tested in preclinical studies. Modulating tumor mechanics with therapeutic agents is emerging as a new research direction for cancer nanomedicines,[47–49] and has become a hot topic in the field of cancer therapy in recent years.[42,50,51]

In this review, we mainly discuss nanomedicines that can modulate mechanical stiffness, solid stress and IFP with a focus on how nanomedicines change these abnormal mechanical properties, promote drug-delivery efficiency and enhance antitumor efficacy. We first introduce the formation, characterizing methods and biological effects of these mechanical properties. Conventional modulation strategies will be briefly summarized. Then, we highlight nanomedicines capable of modulating the TMME for augmented cancer therapy. Finally, current challenges and future opportunities will be discussed.

Tumor mechanical microenvironment

Tumor mechanics has recently been recognized to play a crucial role in not only mediating cancer progression but more importantly affecting therapeutic effects of various cancer therapies, including chemotherapy, radiotherapy, targeted therapy, photodynamic therapy and immunotherapy.[1] Compared with normal tissues, the TMME is aberrant (Fig. 1). Overactivated cancer-associated fibroblasts (CAFs), which deposit and crosslink ECM proteins, stiffen tumor tissues.[52] Rapid proliferation of cancer cells, accumulation of ECM proteins and contraction of both CAFs and cancer cells compress normal tissues, resulting in massive solid stress stored in tumors.[5,53] Highly compressed and leaky tumor vasculature and defunct lymphatic vessels lead to increased IFP in tumor tissues.[54] These abnormal properties interact with each other and synergistically exert negative effects on cancer therapy. Abnormal mechanical properties not only accelerate tumor occurrence, development, invasion and metastasis by transmitting mechanical signals,[5,11,55,56] but also form physical barriers that prevent drug delivery and reduce immune cell infiltration into tumor parenchyma.[57–60] In this section, we briefly introduce the definitions, causes, and detection of mechanical stiffness, solid stress and IFP associated with the TMME. The effects of these mechanical abnormalities on tumor progression and cancer therapy are also discussed.

Mechanical stiffness

Mechanical stiffness, or elastic modulus, is defined as the resistance of a material to deformation under the action of quasi-static forces. Macrocosmically, the stiffness of tumor tissue is heterogeneous (Fig. 1). Some studies show that tumor cells are soft while ECM is stiff by investigating biopsy samples from breast, liver and brain cancer patients using atomic force microscopy (AFM).[61–64] Tumor cells are softer than nonmalignant cells due to the changes in their cytoskeletal structure,[65,66] which would enhance the cellular compliance, improve the resistance to shear flow and promote tumor metastasis.[65,67] Although tumor cells are softer than normal cells, tumor tissues are often highly fibrotic, which makes the whole tumor exhibit a stiffer property than normal tissues.[68] Deposition, cross-linking and reconstruction of ECM are the main causes of tumor stiffening. In highly fibrotic tumors, CAFs play a key role in tumor stiffening as the ECM components are mainly produced by CAFs.[69] For instance, collagen, a major component of ECM secreted by CAFs, can be cross-linked by lysyloxidase and transglutaminase 2, resulting in increased tumor stiffness.[69,70] Mechanical stresses can also enhance the stiffness of ECM through strain-stiffening. Both the tensile stress caused by cell contraction or increased tumor volume and the compressive stress resulting from tumor growth would increase tumor stiffness.[53,71,72] Notably, there is a positive feedback loop that further enhances tumor rigidity. ECM stiffening can activate the latent TGF-β and subsequently promote the transformation of fibroblasts into CAFs.[46,69] Meanwhile, the increased tumor stiffness caused by tensile stress can promote contraction of focal adhesion in CAFs, thereby further inducing matrix decomposition and tumor stiffening.[73]

Two methods commonly used to detect tumor stiffness in the clinic are magnetic resonance elastography (MRE) and ultrasound elastography (USE). MRE is a non-invasive imaging technique which uses a combination of sound waves and magnetic resonance imaging (MRI) to measure the elastic properties of tissue, such as differentiating the stiffness of a liver tumor from surrounding healthy and fibrotic tissues.[74–76] By utilizing this technique, researchers are able to diagnose a range of liver diseases, such as hepatocellular carcinoma, cirrhosis, fatty liver, and fibrosis, as well as to evaluate the effectiveness of treatment for these indications.[77] Despite its many advantages, such as the lack of any invasive procedures, the accurate measurement of the liver tumor modulus, and a complete three-dimension (3D) image stack of the tissue displacements, MRE is an expensive and time-consuming procedure due to the need for specialized equipment and an experienced operator.[78,79] USE is also a non-invasive imaging technology

Zifu Li

Professor Zifu Li received his BS degree from the Huazhong University of Science and Technology in 2008 and PhD degree from the Chinese University of Hong Kong in 2012. From 2013 to 2015, he worked as a postdoctoral fellow at the University of Alberta. He then joined the Georgia Institute of Technology as a research scientist. Since 2016, he has been a full professor at Huazhong University of Science and Technology. His group studies mechano-nanooncology, hyperbaric oxygen-enabled cancer therapy and smart nanomedicines.
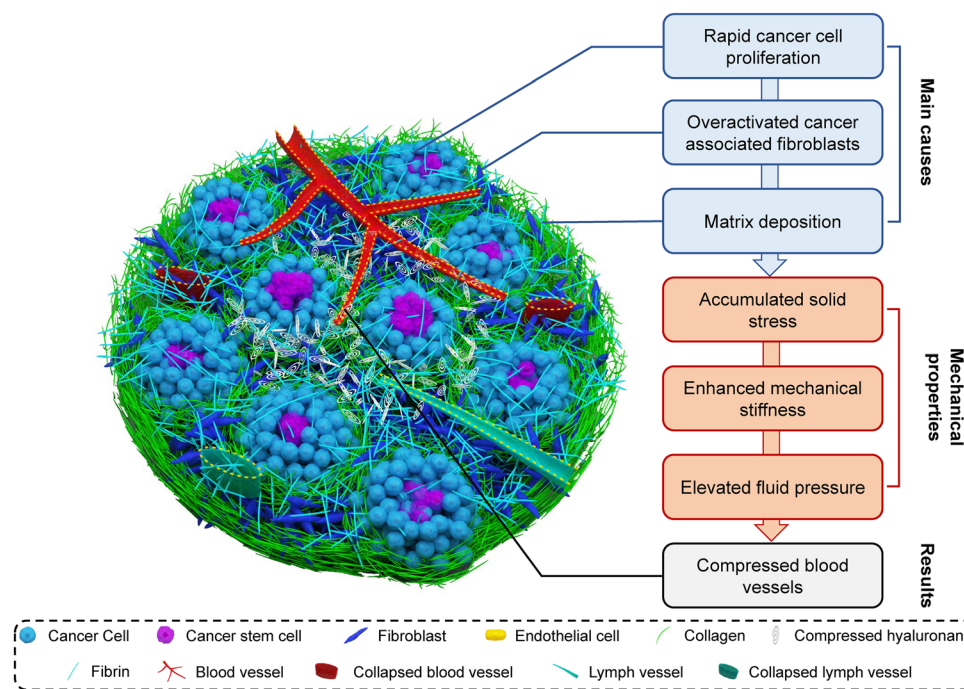
Fig. 1 Causes and results of abnormal tumor mechanical microenvironment. Rapid cancer cell proliferation, overactivated cancer-associated fibroblasts (CAFs), and excessive extracellular matrix (ECM) deposition contribute to perpetuating an abnormal tumor mechanical microenvironment. This aberrant microenvironment leads to a series of unfavorable events that include but are not limited to the accumulation of solid stress, enhanced mechanical stiffness, and elevated interstitial fluid pressure (IFP), which are considered the main culprits responsible for compressing blood and lymphatic vessels.

for preoperative pathological diagnosis, such as liver fibrosis assessment or breast lesion characterization. USE can also be utilized in tissue stiffness testing by measuring tissue strain. The principle is that tissues produce strains under the applied pressure during the exploration, and the strain is smaller in a stiff area than that in a soft area.[80] Recent clinical studies,[3] using USE, estimate an average elastic modulus of 5 kPa for healthy liver, and in excess of 20 kPa for advanced liver cancers. USE measurements also show that the average stiffness of normal pancreatic tissue is only 2.5 kPa, but the average stiffness of pancreatic cancer tissue is 6.1 kPa.[4] USE holds immense potential for various clinical applications in the liver, breast, thyroid, kidneys, prostate, and lymph nodes. Nonetheless, there are still many inherent limitations that hinder the reproducibility of USE measurements (Table 1). A number of these can be attributed to shadowing, reverbera-

Table 1 Common methods for detecting tumor mechanical properties

TMME traits	Methods	Advantages	Limitations	Refs
Stiffness	Magnetic resonance elastography	Full 3D image of tissue and large, movable deeper fields of view and *in vivo*	Expensive and time-consuming procedure	78
	Ultrasound elastography	Non-invasive and rapid	Low detection accuracy for complex tumor structure	80
	Atomic force microscopy	High-resolution and continuous mapping	Cannot map the interior of a tissue; require slicing, require physical contact and *in vitro*	53
	Unconfined compression test	High detection accuracy	Lack of stresses in other two planes of 3D, *in vitro*	86
Solid stress	Tumor-opening	Simple and rapid	*In vitro* and only suitable for tumors with certain volumes	58
	Planar-cut	Large dynamic range of solid stress estimation	*In vitro*, require agarose and consecutive cuts	53
	Slicing	A wide range of specimen sizes, sufficient stress release	*In vitro*; require agarose and consecutive cuts	53
	Needle-biopsy	*In situ*	Traumatic	105
IFP	Wick-in-needle	*In vivo*, simple and rapid	Insufficient detection depth	115
	Micro puncture	*In vivo*, deeper areas, simple and rapid	Traumatic, controversial pressure calibration	117

tion, and clutter artifacts, or the operator-dependent nature of free-hand ultrasound systems.[81] Besides, the complex architecture and high tissue anisotropy of tumors can also result in erroneous measurements. In fact, due to the above limitations, it is only recommended to distinguish significant or advanced fibrosis from non-significant fibrosis by USE.[82]

The stiffness of tumor tissues can also be quantified through AFM measurement (on the microscale) and unconfined compression test (UCT) (on the macroscale).[53] AFM measures the tumor tissue stiffness by deflection of the cantilevers caused by the repulsive force between the probe and the sample. Notably, for AFM measurements, tumor tissues should be prepared as a thick slice and measured within 2–3 h.[83] More useful information on characterizing tumor tissue mechanical stiffness can be found elsewhere in excellent reviews.[84,85] UCT is another reliable and effective method for measuring the stiffness of tumor tissues. To use this method, slices of freshly excised tumor tissue are placed in an unconfined compression chamber submerged in phosphate buffer solution (PBS). The chamber is then mounted in an ultrasensitive servo-controlled materials tester and the specimen is compressed by 5% of the original height in ramps of 20 seconds. After allowing the specimen to relax for about 20 minutes, Young's modulus is determined as the ratio of the linear fit to the stress–strain data.[86,87] Despite the accuracy of this method, there are still certain limitations that need to be taken into consideration when using UCT (Table 1). We can only detect the stress component at the cut surface, while the 3D stiffness heterogeneities of tumor tissues cause a lack of stresses in the other two planes. Whether living tumor tissue's mechanical stiffness can be fully detected by UCT is still an unresolved issue. Nevertheless, UCT represents a powerful tool for measuring the mechanical stiffness of tumor tissues. Compared with MRE and USE, AFM and UCT have the advantages of higher detection accuracy. Nonetheless, AFM and UCT cannot obtain the mechanical stiffness of tumor tissues *in situ* and *in vivo*. Tumor tissues must be excised from cancer patients in the clinic, or from mice in preclinical studies. Furthermore, only the mechanical stiffness of cutting plane is attainable by AFM and UCT, while 3D mechanical stiffness distribution can be obtained by MRE and USE.

Mechanical stiffness exerts profound impacts on tumor progression and cancer therapy. An *in vitro* study revealed that mammary epithelial cells can differentiate into acinus when they are cultured in a condition that simulates the stiffness of breast tissues.[88] EMT can occur in mammary epithelial cells with increased matrix stiffness. These cells lose their cell–cell adhesion and apical–basal polarity, and acquire the abilities to invade and metastasize. Other research draws the same conclusion, that human colon cancer cells can exhibit a metastatic-like phenotype when they are cultured on substrates with raised mechanical stiffness.[89,90] The increased tumor rigidity can increase the degree of malignancy as well.[91–94] For pancreatic cancer, the elevated pancreatic stiffness indicates the enhanced invasion and metastasis capacity of pancreatic cancer cells.[93] Hyper-fibrotic pancreatic tissue not only pro-

motes the EMT process but also reduces the chemosensitivity of pancreatic carcinoma cells to paclitaxel (PTX).[94] Mechanical stiffness also regulates tumorigenesis and tumor development by transforming physical signaling into biochemical signaling through mechanical transduction pathways. For example, the alteration of tumor stiffness can be sensed by integrins, which subsequently activate focal adhesion kinase (FAK)-mediated signaling transduction.[95] Yes-associated protein (YAP) can be activated by the stiff matrix and then mediates cellular signaling transduction through actomyosin, Rho-associated protein kinase (ROCK) and Src, thereby maintaining and enhancing the function of CAFs.[96,97] Furthermore, TGF-β mediates mechanical signaling transduction through various signaling pathways in stiff matrix.[98] In conclusion, increased tumor stiffness can promote the secretion of cell growth factors, cellular signaling transduction and induce EMT, leading to enhanced tumor metastasis and malignant degree, and reducing the chemosensitivity of cancer cells.

Solid stress

Solid stress refers to the mechanical force stored in or transmitted through ECM and cells, including compressive stress, tensile stress and shear stress.[99] By definition, solid stress is distinct from mechanical stiffness. Jain *et al.* elegantly demonstrated that tumor solid stress increased with tumor growth whereas tumor mechanical stiffness was independent of tumor size.[53] Tumor solid stress is generated in the following ways. First, tumor cell proliferation and matrix deposition increase tumor volumes, which compress the viscoelastic structural units inside and outside tumor tissues, generating solid stresses towards tumors and surrounding tissues.[53,72] Second, tumor invading normal tissue produces solid stress.[100,101] For solid tumors with well-circumscribed nodular masses, considerable solid stresses would be generated when tumors push the surrounding tissues. Nevertheless, for invasive tumors with an infiltrating phenotype, relatively small solid stresses would be generated when tumors grow in normal tissues.[72,102] Third, swelling of the glycosaminoglycan matrix components by absorbing water would generate solid stress.[86] Fourth, cell contractions mediated by actomyosin could produce solid stress as well.[103]

Measuring tumor opening is a simple technique that can rapidly test solid stress. The seminal work of Jain *et al.*[58] determined that the solid stress in the interior of murine tumors ranged from 0.37 to 8.01 kPa, which was consistent with their earlier works on solid stress measurement by using cutting experiments and model predictions.[58,104] In this method, approximately 80% of the thickness is cut along the longest axis of the tumor, and the stress relaxation was evaluated as the extent of tumor opening normalized to the diameter of the tumor. The solid stress value was then calculated according to the mathematical model and the estimated material properties of tumor tissue. It predicted that the compressive stress was distributed in the center of the tumor, while the tensile circumferential stress was distributed at the edge of the tumor.[13] Measuring tumor opening for solid stress detection has its

own limitations (Table 1). First, this method is only suitable for testing the solid stress of stiff tumors with certain volumes. When applied to soft or small tumors, the tumor incision might be difficult to open due to the insufficient releasing stress in the tumor. Besides, the tumor opening test can only be carried out *in vitro*, which means that clinical application of this method is difficult. Unlike tumor stiffness that can be mapped *in vivo* and *in situ*, developing reproducible and objective methods for solid stress measurement *in vivo* has been challenging. To further characterize tumor solid stress, Jain *et al.* developed three other methods (planar-cut, slicing, and needle biopsy).[53,105] The planar-cut is a method used to characterize solid stress by cutting a tumor along a plane parallel to the tumor surface. This type of sampling allows researchers to measure the amount of stress present in the tumor from a 3D perspective. This method provides an indication of the amount of stress present in the tumor. The planar-cut is a valuable tool for researchers studying the effects of stress on tumor growth and progression. The slicing is a method used to quantify solid stress by cutting a sample into thin slices. This type of sampling allows researchers to measure the amount of stress present in the tumor from a two-dimensional viewpoint. Needle biopsy is a procedure in which a small sample of tissue is removed from a tumor for diagnostic testing. This type of biopsy can help characterize the tumor's solid stress by measuring the physical characteristics of the tumor, such as its shape deformations in excised tumor tissues and original tissues. These methods can be applied to a variety of malignant solid tumors such as breast cancer, pancreatic cancer, brain cancer, and colon cancer.[105] In these operations, the solid stress of the tumor is released in a controlled manner, then the incision deformation is reconstructed by ultrasound imaging technology, thus the solid stress and elastic potential energy of the tumor can be calculated by finite element modeling. It was found that solid stress increased with tumor size, but the stiffness did not. This suggested that the effects of solid stress and stiffness on tumor tissue and cell behavior should be considered independently. These methods have non-negligible shortcomings (Table 1). The planar-cut and the slicing are limited to *ex vivo* measurements and require embedding of the tissues in agarose before cutting. The current controversy is whether mechanical cutting or slicing can reflect tumor solid stress practically, for some residual stress may still remain and cannot deform the tumor after solid stress is released. Therefore, how to measure solid stress in a non-invasive manner with the help of existing clinical testing instruments and technologies needs further investigations.

Tumor solid stress plays an important role in tumor progression and cancer therapy. Solid stress compresses tumor blood and lymphatic vessels,[58,106,107] which hampers oxygen and drug delivery through blood vessels, resulting in tumor hypoxia, decreased immune cell infiltration, formation of an immunosuppressive microenvironment, and reduced antitumor effects.[57-60] In addition, tumor solid stress affects tumor biology through a variety of pathways. First, solid stress can directly affect cells through applying forces on intercellular adhesion, cell–ECM adhesion and stretch-sensitive ion channels.[60,108,109] Second, solid stress can modulate the nuclear import of transcription factors by affecting the activity of nuclear pore complexes and associated proteins.[5,110] For instance, nuclear deformation caused by solid stress can activate the YAP/transcriptional coactivator with PDZ-binding motif (TAZ) signaling pathway, thereby promoting cell proliferation, inhibiting cell apoptosis, regulating the cell cycle, enhancing the function of cancer stem cells (CSCs), and activating CAFs.[111] Third, solid stress can indirectly affect cancer cells by deforming ECM components. For example, myofibroblasts stretching ECM can activate the latent TGF-β, which can subsequently regulate cancer cells and ECM. Moreover, the tensile forces can induce the unfolding of fibronectin in ECM, elevate the enzymatic resistance of collagen, and regulate the interactions of fibronectin and collagen.[112-114] In summary, solid stress not only contributes to the formation of the TMME and insufficient drug delivery by compressing blood vessels and lymphatics, but also promotes tumor progression and increases the degree of malignancy through regulating cellular signaling pathways by directly affecting mechanosensitive cellular components or indirectly inducing deformation of ECM components.

Interstitial fluid pressure

The third mechanical abnormality of solid tumors is elevated extravascular hydrostatic pressure, also known as interstitial fluid pressure (IFP), which is caused by leaky blood vessels and a compromised lymphatic drainage system.[8] Subcutaneous IFP was first measured in anesthetized rats with the wick-in-needle (WN) technique.[115] In this approach, the wick is placed inside a hypodermic needle with a 2 to 4 mm-long side hole, and is connected to a pressure amplifier and recorder through a polyethylene tube.[116] Results were recorded on a recorder, with a sensitivity of 2 mm of deflection per mm Hg. The WN technique represents a simple and rapid method for measuring IFP. However, the needle tip is easily obstructed, and the continuous water column between the tissue fluid and the needle cavity can be disturbed, which leads to unstable pressure recording. Besides, this technique is traumatic, which might change local IFP (Table 1). There is also no direct evidence to show that the control pressure or the pressure changes accurately reflect the conditions in undisturbed interstitial fluid. Another approach for IFP detection is the micro puncture (MP) technique. Using micropipettes with tip diameters ranging between 2 and 4 μm, Jain *et al.* demonstrated for the first time that IFP was elevated throughout the mammary adenocarcinoma and dropped sharply to normal values at the periphery of the tumor.[117] In this method, zero pressure is calibrated by determining the linear relationship between imposed pressure and measured pressure in a saline test chamber. Individual pressure measurements are made by introducing micropipettes perpendicularly from tumor surface to depths of 2.5 to 3.5 mm and then retracting them back to the surface. Results showed that the average IFP of mammary

adenocarcinoma was 103 mm Hg, and no significant correlation was found between tumor mass and IFP. Nevertheless, these methods have their inherent shortcomings in application. Depth of penetration is the main limitation of the MP technique (Table 1). The MP technique was often used to measure IFP in the superficial layers, while the WN technique was generally utilized to determine IFP in the deeper areas. Furthermore, a common drawback of these two methods is that introduction of a wick in subcutaneous tumor tissues will cause a leakage of albumin from blood plasma into the wick, which would affect liquid pressure measurement to a certain extent. Besides, the WN technique can only test one or two small areas (5 mm × 5 mm) within a tumor, which also narrows its scope of application (Table 1).

Elevated IFP promotes tumor interstitial flow, exposing cells to shear stress. Shear stress has a significant impact on the biology of tumor cells and stromal cells in several ways, including activating CAFs, affecting tumor angiogenesis and lymph angiogenesis, inducing matrix metalloproteinase activation, affecting cell mobility, promoting cancer cell migration and invasion, resulting in cell cycle arrest, and regulating immune cells.[118–122] The above impacts are mainly caused by mechanical signaling transduction mediated by focal adhesions, cell glycocalyx, cell–cell junctions, ion channels and Notch receptor.[7,123,124] These mechanical signals can up-regulate the expression of TGF-β and induce the activation of YAP/TAZ pathways.[118,125,126] The increased IFP can also indirectly affect tumor progression and cancer therapy. The formed fluid pressure gradients can make the interstitial fluid flow from tumor interior to tumor surrounding, which will spread cancer cells and growth factors to the adjacent tissues and lymphatic vessels, thereby contributing to tumor growth and tumor metastasis.[119] Moreover, the increased IFP can impair drug penetration and distribution in tumors, and reduce drug retention time.[10] Overall, the elevated IFP not only affects tumor progression and promotes tumor metastasis through direct or indirect effects, but also hinders drug permeability and retention in tumors, severely restricting the antitumor effect of conventional cancer therapy.

Conventional TMME modulation strategies

As mentioned above, abnormal mechanical properties not only promote tumor progression but also severely limit drug delivery efficiency and antitumor efficacy. Thus, modulating the TMME is essential for potent cancer therapy. Blocking the synthesis of ECM components by small-molecule drugs, including losartan, tranilast and pirfenidone (PFD), decomposing existing ECM proteins by utilizing proteolytic enzymes, like hyaluronidase and collagenase,[127] and suppressing CAFs with hyperbaric oxygen (HBO) therapy are three widely used strategies for regulating tumor mechanics. In this section, we will discuss these conventional TMME modulation strategies for enhanced cancer therapy (Table 2).

TMME modulation by blocking the TGF-β signaling pathway

Losartan, an angiotensin receptor II antagonist, is clinically used to treat hypertension. Some studies illustrated that blocking angiotensin signaling by losartan could inhibit the activation of fibroblasts and reduce ECM contents in

Table 2 Conventional strategies for modulating the TMME to boost cancer therapy

Method	Mechanisms	Drugs	Stages	TMME modulation and therapeutic effects	Ref.
TGF-β signaling inhibition	Suppress ECM synthesis	Pirfenidone, doxorubicin	Preclinical	Elastic modulus decreased by 30% Collagen I and HA decreased by 78% and 71%	133
		Losartan, doxorubicin	Preclinical	Solid stress decreased by 50%, survival prolonged by 200%	59
		Losartan, FOLFIRINOX	Phase 2	Downstaging of locally advanced pancreatic ductal adenocarcinoma Plasma TGF-β concentration decreased by 34%	130
		Tranilast, Doxil	Preclinical	Solid stress decreased by 65%, elastic modulus decreased by 60% IFP decreased by 40%	131
ECM degradation	Degrade ECM components	PEGPH20, gemcitabine	Preclinical	IFP decreased by 75% and enhanced antitumor efficacy	14
		PEGPH20, nab-paclitaxel and gemcitabine	Phase 3	Median PFS prolonged by 76.9% and OS prolonged by 35.3%	137
		PEGPH20, FOLFIRINOX	Phase 2	Median PFS decreased by 44.1% and median OS decreased by 87%	138
Hyperbaric oxygen therapy	Suppress CAFs	Doxil	Preclinical	Decreased collagen deposition with TIR of 91.5%	26
		Abraxane and gemcitabine	Preclinical	Young's modulus decreased by 72.6% Tumor vessel and the vessel tortuosity decreased by 53.7% and 58.5%	30
		Abraxane or Doxil	Preclinical	Solid stress decreased by 40%, suppressing CSCs and cancer metastasis	27
		PD-1 antibody	Preclinical	Solid stress reduced by 40%, PD-1 antibody and CD8^{+} T cell infiltration increased	29
		PD-1 antibody	Phase 1	In progress	29

tumors.[128,129] In the breast cancer E0771 tumor model and pancreatic cancer AK4.4 tumor model, losartan treatment significantly reduced intratumoral collagen (40% for E0771 and 50% for AK4.4) and hyaluronan (HA) contents (10% for E0771 and 25% for AK4.4).[59] Accordingly, solid stresses, as quantified by the tumor opening method, were significantly decreased in both tumor models (50% for E0771 and 50% for AK4.4), while perfused blood vessels were increased by 43% and 45%, respectively. It is worth noting that losartan has no effect on vessel density, but increased the amount of perfused blood vessels in this research, demonstrating that restraining the synthesis of ECM components and relieving solid stress would decompress blood vessels. As a result, losartan treatment markedly improved oxygen and drug delivery to tumor tissues.[59] The combination of losartan and chemotherapeutic agents significantly prolonged the survival of tumor-bearing mice (200% for E7701 and 150% for 4T1 tumor models) (Table 2). In a phase II clinical trial (clinical trial number: NCT01821729), losartan was utilized in combination with neoadjuvant FOLFIRINOX (fluorouracil, leucovorin, oxaliplatin, and irinotecan) and chemoradiotherapy to improve the R_0 resection rate in patients with locally advanced pancreatic cancer.[130] The inspiring results were that the R_0 resection was 61% among all enrolled patients (49) and 88% in the patients that received resection. It was also found that plasma TGF-β levels decreased significantly post treatments with losartan, FOLFIRINOX and chemoradiotherapy, suggesting that losartan might augment the antitumor efficacy of FOLFIRINOX and chemoradiotherapy by interrupting tumor mechanics. These pioneering studies emphasize that modulating the TMME by losartan is beneficial for cancer therapy not only in animal tumor models but more importantly in patients with lethal solid tumors.

Administration of tranilast can achieve similar results as losartan treatment. Tranilast is a commonly used antifibrotic drug in clinical practice. In breast cancer 4T1 and MCF10CA1a tumor models, the intratumoral collagen contents were reduced by 20% and 25%, respectively, and the intratumoral HA contents were reduced by around 40% and 63%, post tranilast treatment (Table 2).[131] With the decrease of matrix components, tumor mechanical properties were improved. Tumor solid stresses of these two tumor models decreased by 35% and 46%, while tumor stiffnesses decreased by 54% and 61%, as measured by UCT. Concurrently, the compression of the tumor vessels was relieved. Researchers found that vessel diameters increased by 10%, and the fraction of perfused blood vessels was enhanced by 50%. Therefore, tranilast treatment could effectively deliver drugs with various diameters, including DOX (<1 nm), Abraxane (10 nm) and Doxil (100 nm), and significantly improve the antitumor effect of traditional chemotherapy and commercialized nanomedicines. Another study also showed that interfering with the mechanical properties of lung metastases by tranilast can alleviate tumor hypoxia and promote drug delivery.[132] PFD is another antifibrotic drug widely prescribed in the clinic, and is generally used for the treatment of idiopathic pulmonary interstitial fibrosis.[133] In 4T1 and MCF10CA1a tumor models, PFD reduced the amount of HA and collagen in tumors via mediating the TGF-β signaling pathway. The investigators further demonstrated that both tranilast and PFD were capable of reducing solid stress (as measured by tumor opening) and mechanical stiffness (as characterized by UCT).[134] These studies corroborated that the accumulation of ECM components, including HA and collagen, were responsible for the aberrant TMME. However, the relationship between solid stress and mechanical stiffness is unclear.

TMME modulation by enzymes degrading ECM components

Hyaluronidase can decompose intratumoral HA and reduce the degree of tumor fibrosis, thereby interrupting tumor mechanical properties. A study showed that pegylated recombinant human hyaluronidase (PEGPH20) combined with GEM could significantly prolong the survival of mice with pancreatic ductal carcinoma.[14] The reason is that PEGPH20 degrading intratumoral HA could significantly reduce IFP in tumors. The IFP of pancreatic ductal carcinoma reduced by 75% after PEGPH20 + GEM combination treatment relative to GEM single treatment. Besides, tumor tissues with PEGPH20 + GEM treatment became soft and the diameters of vessels increased significantly. These changes are conducive to GEM delivery to tumor tissues. However, the operational mechanism for PEGPH20 on pancreatic tumor blood vessels has aroused considerable debate. Adopting the MN technique, it was found IFP in pancreatic tumors was much smaller than that measured by the piezoelectric probe technique.[135] The authors reasoned that the piezoelectric probe technique indeed detected both IFP and solid stress. Therefore, it was suggested that PEGPH20 decompressed pancreatic tumor blood vessels by reducing solid stress rather than IFP. Despite these controversies, PEGPH20 has been tested together with standard therapies for pancreatic cancers in numerous clinical trials.[136–138] In one trial, PEGPH20 was combined with nab-paclitaxel/gemcitabine for the treatments of patients with untreated metastatic pancreatic ductal adenocarcinoma (PDAC). Although significant benefits in progression-free survival (PFS) were exhibited in the phase II trial,[137] no evident advantage was observed for overall survival (OS) in the subsequent phase III trial. Even worse, the addition of PEGPH20 to mFOLFIRINOX was demonstrated to be harmful for patients with metastatic PDAC in another phase IB/II trial.[138] The combination of PEGPH20 with mFOLFIRINOX reduced median OS and increased toxicity. It should be noted that no tumor HA status was selected in this trial. These clinical trials highlight the differences between preclinical models and cancers in patients, and underscore the need for more fundamental studies on mediating the TMME for cancer therapy.

TMME modulation by hyperbaric oxygen therapy

HBO therapy can effectively interfere with the TMME and augment therapeutic effects by overcoming tumor hypoxia and inhibiting CAFs.[30] HBO is a treatment where patients breathe pure oxygen at 2 to 3 atmospheric pressures. HBO treatment is

safe and has been widely utilized in treating ischemia, acute carbon monoxide poisoning, unhealed wounds and radiation injury.[139,140] Currently, HBO treatment is considered as one of the most effective means of delivering oxygen to solid tumors.[141] HBO treatment can directly increase the oxygen concentration in plasma, without relying on hemoglobin-based oxygen delivery.[142] Therefore, HBO exhibits outstanding oxygen delivery efficiency as compared with other strategies. Multiple studies that combine HBO with conventional antitumor treatments have been reported in recent years.[26,27,29,30] By suppressing CAFs, blocking ECM-related gene expression, and reducing the ECM contents in tumors,[30] HBO treatment significantly mediated tumor mechanical properties and boosted antitumor effects.[29,30] In the pancreatic Panc02 tumor model, study showed that hypoxia promoted the proliferation of CAFs and synthesis of ECM components, while HBO treatment could inhibit the proliferation of CAFs through curbing TGFβ1 secretion from Panc02 tumor cells.[30] After treatment with HBO, the contents of total collagen, collagen I and fibronectin in pancreatic tumor-bearing mice were reduced by 37.5%, 42.5% and 40.4%, respectively (Table 2). With the decrease of ECM contents, the mechanical stiffness of pancreatic tumor (as detected by AFM) reduced by more than 50%. Besides, tumor vessels were normalized and vessel tortuosity was diminished by 58.5%, leading to an enhanced delivery efficiency of Abraxane to tumor tissues. With HBO treatment, the accumulation of Abraxane in tumors was around 1.7 times as much as that of the control group, and the drug penetration depth and cellular uptake were 3.78 and 1.82 times higher than in mice without HBO treatment. Therefore, combination treatment of HBO and abraxane/gemcitabine (GEM), the first-line treatment for pancreatic cancers, significantly improved the tumor inhibition effect and anti-metastasis efficacy. In the triple-negative breast cancer (TNBC) 4T1 tumor model, alleviating the hypoxia microenvironment could also deplete excessive ECM and interfere with tumor mechanical properties.[27] After treatment with HBO, the contents of collagen and fibronectin in 4T1 tumors were reduced by 41% and 65%, respectively. Meanwhile, 4T1 tumor solid stress decreased by approximately 40% as revealed by tumor opening. As a result, compression of tumor blood vessels was significantly relieved while blood perfusion (as measured by laser speckle blood flow imager) was significantly improved. This study demonstrated that HBO modulating the TMME dramatically enhanced drug accumulation of Abraxane (by 36%) and Doxil (by 25%) and increased the penetration depth of Abraxane (by 3.86-fold) and Doxil (by 4.42-fold), thereby effectively eliminating cancer stem cells (CSCs). Additionally, in the hepatocellular carcinoma (HCC) H22 tumor model, decreasing ECM components and improving the TMME by HBO treatment increased the vascular extravasation and tumor penetration depth of program death-1 (PD-1) antibody by 2.6 times.[29] This study also showed that HBO treatment significantly increased T-cell infiltration in tumor parenchyma and promoted the antitumor effects of ICB immunotherapy against both rodent tumor cells and cancer cells derived from fresh tumor tissues excised from cancer

patients with HCC. The combination of HBO and PD-1 antibody is currently being tested in a single-arm clinical trial (NCT05031949) in patients with HCC. In another clinical trial, HBO was combined with nab-paclitaxel/gemcitabine for the treatment of patients with pancreatic cancers. The above studies collectively corroborate that HBO treatment can reduce tumor rigidity, relieve tumor solid stress, decompress tumor blood vessels, and improve blood perfusion by overcoming tumor hypoxia, suppressing CAFs and inhibiting the synthesis and secretion of ECM components, in varieties of tumor models. These effects have been proved to be beneficial for boosting the therapeutic efficacy of commercialized nanomedicines and PD-1 antibody-based immunotherapy. Therefore, mediating tumor mechanical properties by HBO is of great significance for clinical applications. Despite these studies, the mechanism by which HBO inhibits CAFs is unclear and calls for further fundamental studies. As CAFs are heterogeneous both phenotypically and functionally and can be divided into at least three subtypes,[69] namely, myofibroblastic CAFs, inflammatory CAFs, and antigen-presenting CAFs, it is not clear yet which subpopulation of CAFs is affected the most by HBO.

While it is true that many conventional treatments such as HBO can modulate the TMME, determining which strategy works best and has the most clinical value depends on several factors, such as the specific type and stage of cancer, the overall health of the patient, and the goals of the treatment. For instance, the conventional therapeutic modality of hyperbaric oxygen confers distinctive advantages, including its non-invasive nature and the potential to modulate the mechanical properties of tumors situated beyond the surface layer. Notwithstanding the promising therapeutic potential of hyperbaric oxygen, its clinical application is not without limitations. Patients who present with high or low blood pressure, respiratory infections, and concurrent active bleeding may be ineligible for treatment due to contraindications.

Nanomedicine-based TMME modulation for cancer therapy

With recent advances in nanotechnology and tumor mechanobiology,[1,5,11,16] nanomedicines that target the TMME have received tremendous attention.[47,49] As fast-growing cancer cells, overactivated CAFs, and excessive ECM components are the main causes for abnormal TMME,[13] including accumulated solid stress, promoted mechanical stiffness and elevated IFP (Fig. 1), which are deemed as the main physical barriers for drug delivery, nanomedicines are rationally designed for augmented cancer therapy. In this section, we briefly introduce four nanomedicine-based TMME modulation strategies (Fig. 2), including metronomic therapy, photothermal therapy (PTT), photodynamic therapy (PDT), and combination therapy. We showcase representative examples (Table 3) and elaborate the TMME-modulation mechanism and their effects on drug delivery, tumor immune environment and therapeutic outcomes.
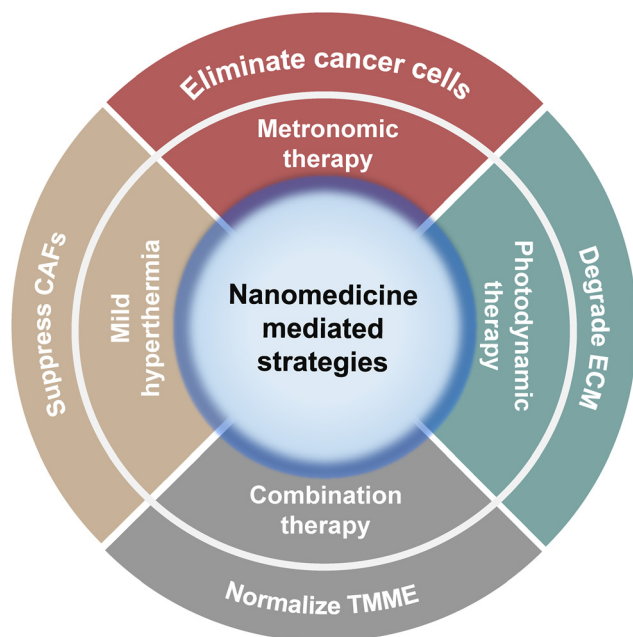
Fig. 2 Physical hallmarks of the TMME as targets for nanomedicine to boost cancer therapy.

Nanomedicine-based metronomic therapy

Metronomic therapy regulates the TMME by eliminating cancer cells. By using a lower and more frequent dose schedule than standard therapy, metronomic therapy can maintain the plasma drug in a relatively low but effective concentration range for a longer time. Therefore, metronomic therapy can reduce the side effects and prolong the survival of patients, and has become an attractive alternative to maximum tolerated dose (MTD) treatment.[143–145] Some studies pointed out that metronomic therapy, by killing cancer cells, not only improved antitumor effects, but also normalized the TMME, improved the function of tumor blood vessels[146] and reversed tumor immunosuppression as compared with MTD treatment.[145,147] Nanomedicines can also maintain the plasma drug concentration in a relatively low but effective range for a long time, owing to their long circulation time and controlled drug-release capacity.[148] Thus, nanomedicines can induce similar cascade effects as metronomic therapy.[149] A recent study showed that Doxil can modulate the TMME and enhance the antitumor effect of ICB immunotherapy.[149] In detail, Doxil treatment with a lower and more frequent dose schedule (1 mg kg^{-1}, daily for six days; 2 mg kg^{-1}, every other day three times a week) exerted a higher tumor-suppression rate than MTD treatment (6 mg kg^{-1}, once a week). In this study, the authors demonstrated that nanomedicine-based metronomic therapy could decompress tumor blood vessels and enhance blood perfusion (as detected by dynamic contrast-enhanced ultrasound) by reducing mechanical stiffness (as measured by ultrasound shear wave elastography), solid stress (as revealed by tumor opening), and IFP (as probed by the WN technique) (Table 3), thereby increasing the infiltration of immune cells (natural killer cells and CD8$^+$ T cells) in tumor tissues and inducing the transition of M2-like tumor-associated macrophages (TAMs) to M1-like TAMs.[149] The above study indicates that administering nanomedicine for metronomic therapy is an effective strategy for tumor mechanics modulation and immunotherapy promotion. Compared with small molecular drugs,

Table 3 Nanomedicines that interrupt the TMME to boost cancer therapy

Method	Mechanisms	Drugs	Stages	TMME modulation and therapeutic effects	Ref.
Metronomic therapy	Eliminate cancer cells	Doxil	Preclinical	IFP decreased by 83% and elastic modulus decreased by 50%	149
Mild hyperthermia	Suppress CAFs	FDINs	Preclinical	Young's modulus decreased by 70%, solid stress decreased by 30% Eliminated CSCs and achieved a TIR of 86%	38
		CHI	Preclinical	Young's modulus decreased by 36%, solid stress decreased by 43 Inhibited CSCs and achieved a TIR of 72%	37
		mP	Preclinical	Young's modulus decreased by 47%, solid stress decreased by 25% Suppressed homologous recombination repair pathway and achieved a TIR of 86%	39
Photodynamic therapy	Degrade ECM	UNPSs	Preclinical	Collagen I decreased by 35% and inhibited tumor growth	28
Combination therapy	Normalize TMME	Tranilast, Doxil and ICB	Preclinical	Decompressed blood vessels in lung metastasis and restored blood perfusion Achieved potent synergistic combination therapy in ICB-refractory breast cancers	132
		Tranilast, epirubicin, Doxil and ICB	Preclinical	Tumor stiffness decreased by 80%, IFP decreased by 50% Increased T-cell infiltration for robust antitumor immune responses	175
		Met@Man-MPs and PD-1 antibody	Preclinical	Decreased collagen I by 70% and facilitated PD-1 antibody delivery Repolarized TAMs and increased CD8$^+$ T cell infiltration	177

the advantages of nanomedicine-based metronomic therapy are that nanomedicines have longer blood circulation time, have fewer adverse effects towards normal organs and tissues, and require less frequent dosing. However, the mechanism by which nanomedicine-based metronomic therapy modulates the aberrant TMME is not yet clear and awaits further investigations.

Nanomedicine-based mild hyperthermia

Mild hyperthermia is an effective strategy for regulating ECM components. For instance, mild hyperthermia can decrease tumor stiffness by affecting the organization of collagen fibers.[46] Collagen fibers may undergo a reversible thermal transition between 31 and 37 °C.[150] However, an irreversible thermal transition will occur within 37 to 55 °C. One study showed that the morphology of collagen changed and the tissue structures were destroyed when tumors were treated with PEG-modified iron oxide nanocubes-mediated magneto-thermotherapy in a human epidermoid carcinoma A431 tumor model.[43] The interfibrillar space increased from 101 to 133 nm. Meanwhile, it was observed that nanocubes accumulated near collagen fibers and infiltrated into tumor tissues after thermotherapy. Another study investigated the distinct effects of mild hyperthermia (43 °C, 15 min) and thermal ablation (52 °C, 3 min) on tumor stiffness by using multi-walled carbon nanotubes (MWCNTs).[45] In the A431 tumor model, researchers found that the effects of mild hyperthermia and thermal ablation on tumor stiffness both exhibited two different stages of characteristics: temporary stiffening of tumor tissues and subsequent continuous reduction of tumor tissues. Owing to the photothermally induced denaturation of protein and necrosis of tumor tissue, the stiffness of tumors increased rapidly within several minutes following the first mild hyperthermia and thermal ablation treatment. The temporary stiffening of tumor tissues was relieved within 24 h and reduced to the original stiffness before treatments. After the second mild hyperthermia and thermal ablation treatment, tumor stiffness decreased continuously. The decrease of tumor stiffness induced by photothermal therapy is mainly related to the reduction of tumor volume, which is caused by the destruction of ECM and apoptosis of cancer cells. Although both mild hyperthermia and thermal ablation treatment effectively destroy collagen and reduce tumor rigidity, thermal ablation will deteriorate tumor blood vessels, which is not conducive to subsequent drug delivery. In contrast, mild hyperthermia treatment is beneficial for improving tumor blood perfusion, increasing the size of tumor capillary pores, and facilitating the exudation of nanomedicines (∼100 nm) from blood vessels to tumor tissues.

While the effects of hyperthermia on ECM proteins and biopolymers have been documented by numerous groups in various tumor models,[151–154] the impacts of mild hyperthermia on CAFs have aroused tremendous interest in the past few years. In light of the significance of CAFs in the aberrant TMME, Li *et al.* developed a hydroxyethyl starch (HES)-based smart nanomedicine (CHI) to target and eliminate CAFs, by using HES-IR780 nanoparticles conjugated with the Cys-Arg-Glu-Lys-Ala (CREKA) peptide, which has a specific affinity for fibronectin overexpressed on CAFs. Upon systemic administration, CHI efficiently targeted CAFs and generated hyperthermia upon light irradiation, thus effectively suppressing CAFs through a photothermal effect. This led to a series of changes in the TMME, including decreases in total collagen, collagen I, fibronectin, tumor mechanical stiffness (decreased by 36%, as probed by AFM), and solid stress (reduced by 56.3%, as revealed by tumor opening), thereby normalizing intratumoral blood vessels, promoting blood perfusion (increased by 40%, as detected by laser speckle blood flow imager), alleviating tumor hypoxia, eliminating CSCs, disrupting the CSC niche, and constraining CSC survival (Table 3).[37] Based on the above findings, the same group explored the effects of mild hyperthermia on CAFs by tumor-targeting HES smart nanomedicine.[38] The investigators harnessed the unique properties of a carbamate disulfide bridged doxorubicin dimeric prodrug as a pharmaceutical ingredient, combined with the therapeutic potential of IR780 iodide as a photothermal agent and biocompatible hydroxyethyl starch–folic acid conjugates as an amphiphilic surfactant, to fabricate an active targeting nanomedicine (FDINs), which binds with folate receptors highly expressed on the surfaces of numerous cancer cells. The photothermal effect of FDINs modulated the aberrant TMME by reducing by 50.1% podoplanin-positive CAFs and depleting by 52.0% collagen I and 49.1% fibronectin of the ECM, thereby decreasing mechanical stiffness by 69% (as probed by AFM) and solid stress by 25% (as quantified by the tumor opening method) (Table 3). Consequently, both the structure and function of intratumoral blood vessels were restored to facilitate oxygen transport (the expression of HIF-1α decreased by 34.8%) and drug delivery (increased by 45%). Furthermore, FDINs is demonstrated to eliminate 27.9% of CD44+CD24− cancer stem cells (CSCs) by disrupting the CAF-mediated CSC niche and depleting intracellular GSH levels within CSCs. Notably, these effects translate into an extra 45% reduction in tumor growth in the 4T1 orthotopic breast cancer model. These inhibitory effects reveal the potential of FDINs as an efficacious therapeutic agent, which is capable of eliminating the most aggressive and treatment-resistant CSC subpopulation in breast cancers.[38] Inspired by the above findings, the same research group further developed a passive targeting nanoparticle, mesoporous polydopamine (mP), for the simultaneous delivery of Olaparib, a typical Poly (ADP-ribose) polymerase inhibitor, and DOX.[39] Study results demonstrated that locally administered mild photothermal therapy (PTT) (with temperatures around 43 °C) exerted a profound impact on the TMME of TNBC. By alleviating tumor hypoxia, suppressing CAFs and reducing the amount of ECM components, mP-mediated mild hyperthermia normalized tumor mechanical stiffness, solid stress, and tumor vasculature (Table 3), thereby enhancing delivery efficiencies of Olaparib and DOX, inhibiting the homologous recombination repair pathway, and augmenting the tumor inhibition rate (TIR) by 26.1%.[39] In this work, the investigators also compared different heating modes

for interrupting the TMME and cancer therapy. It was found that mP-mediated mild hyperthermia was superior to water bath heating in terms of repressing podoplanin-positive (PDPN[+]) CAFs, decreasing ECM contents (including α-SMA and collagen I), and inhibiting tumor growth, emphasizing the significance of nanomedicine-mediated hyperthermia in cancer therapy. At the same temperature of 43 °C, mP-mediated mild hyperthermia achieved a TIR of 85.4% whereas the water bath heating obtained a TIR of 63.7%. As hypoxia promoted CAFs while HBO suppressed CAFs by disrupting tumor hypoxia,[30] the authors proposed a model to account for the impacts of mP-mediated locally mild hyperthermia on the aberrant TMME of TNBC. Upon systemic administration, mP first accumulated at tumor tissues by the enhanced permeability and retention (EPR) effect. Then with the laser light irradiation, mP converted energy from laser light to heating and generated the mild hyperthermia effect, which alleviated hypoxia to suppress CAFs and block ECM production. These effects contributed to decreases in tumor mechanical stiffness and solid stress, thereby normalizing intratumoral blood vessels to facilitate drug delivery and oxygen transport. By comparing the results of CHI, FDINs and mP, it can be seen that is not necessary to prepare sophisticated nanomedicines for targeting CAFs. This conclusion is corroborated by other researchers.[40,41] Nanomedicines with simple structure and components have a higher chance of clinical translation and bedside application. However, molecular understanding of nanomedicine-mediated mild hyperthermia on TMME regulation warrants further investigations.

Nanomedicine-based photodynamic therapy

Photodynamic therapy (PDT) is also a viable strategy for regulating the TMME. PDT is a minimally invasive treatment which mainly utilizes specific wavelengths of near-infrared light or visible light to irradiate photosensitizers (PSs) to produce reactive oxygen species (ROS) and induce cellular or tissue damage at the site of light irradiation.[155] It has been widely applied for cancer therapy, accompanying different functional PSs synthesized, either alone or combined with other treatments.[156–158] PDT with powerful cytotoxicity and exquisite spatiotemporal control capacity makes it an attractive approach that can directly target tumor tissues.[159] In recent years, an expanding array of nanomedicines designed to target the tumor microenvironment using photodynamic therapy have been developed.[28,36] In one particular study, a prostate-specific membrane antigen (PSMA)-targeted bacteriochlorophyll photosensitizer was developed for subtherapeutic PDT, which did not induce significant cancer cell death or vascular destruction but promoted tumor vascular leakage and facilitated tumor accumulation of subsequently administered nanoparticles by regulating ECM content and ultrastructure.[36] As a result, with the help of subtherapeutic PDT, 5 mg kg^{-1} of Doxil achieved a similar tumor inhibition effect as 15 mg kg^{-1} of Doxil. ROS-mediated collagen degradation was also reported with upconversion nanophotosensitizers (UCNPSs),[28] which achieved a robust tumor suppression effect together with

HBO. Nonetheless, the influences of PDT on tumor mechanical properties, including mechanical stiffness, solid stress and IFP, were not investigated in these studies.

While PDT has shown promising results in preclinical and clinical studies, it also has some limitations.[160–162] One of the major limitations of PDT is the limited light penetration depth in tissues, which restricts its use to superficial tumors.[163,164] This limitation can be partially overcome by using near-infrared (NIR) light, which has better tissue penetration.[163,164] Non-specific accumulation is another issue. While PDT can selectively target tumor tissues that have been sensitized with light-sensitive drugs, non-specific uptake of the drugs in healthy tissues can result in damage to healthy tissues and cells.[165] Tumors are heterogeneous in nature, and PDT may not be effective in all parts of the tumor, leading to incomplete treatment and tumor recurrence.[166,167] In summary, while PDT has shown promise as a cancer treatment approach, its effectiveness is limited by several factors, including the limited light penetration depth, non-specific targeting, tumor heterogeneity, and treatment resistance. Furthermore, PDT-mediated TMME regulation mechanisms are far from being revealed and still need substantial research to optimize the use of PDT for cancer treatment.

Nanomedicine-based combination therapy

Although the nanomedicine-based modulation strategies mentioned above have improved the abnormal TMME to some extent and achieved benefits for cancer therapy, the complex pathophysiological characteristics of solid tumors greatly limit the performance of the single therapeutic strategy, especially for immunotherapy.[1,168,169] Cancer immunotherapy aims to enhance the patient's natural immune responses, thereby facilitating the inhibition or eradication of malignant cancer cells.[170,171] The complete process of cancer immunotherapy involves a series of steps. At the outset, cancer cell antigens are released into tumor tissues, triggering the recognition of these antigens by dendritic cells. This leads to the proliferation and activation of T cells, which are capable of responding to cancer cell antigens. As these T cells traffic to tumor sites, they infiltrate into tumor parenchyma, recognize and engage with cancer cells in a specific manner.[172] However, the abnormal TMME once again interferes with many processes, which may reduce the response rates of immunotherapy.[173] For instance, the elevated solid stress and enhanced mechanical stiffness impede dendritic cells from releasing immunogenic signals and presenting antigens, resulting in an immune-desert phenotype.[173] Furthermore, the variable vascular shear stress, excessive ECM, and raised IFP collectively impede the extravasation of T cells from blood vessels and their infiltration into tumor parenchyma, generating an immune-excluded phenotype.[1] These features are mostly interrelated and could serve as new clues to cancer therapy. Appropriate combination strategies are expected to reshape the TMME to achieve higher survival benefits.[174] Here, we discuss the limitations of current immunotherapy resulting from the TMME, and explore the potential of nanomedicine-mediated TMME regulation for augmented immunotherapy.

Antifibrotic drug tranilast, either as free drug or encapsulated within a nanocarrier, has been used together with Doxil to regulate the abnormal TMME for enhanced ICB immunotherapies.[132,175] Stylianopoulos *et al.* revealed that the blood vessels in lung metastases of breast cancer patients are susceptible to mechanical compression.[132] Accordingly, the investigators deftly exploited the therapeutic potential of tranilast, by impeding the biosynthesis of HA and collagen I, to effectively decompress the blood vessels and restore blood perfusion, thereby significantly mitigating the hypoxic state in a model of breast cancer lung metastasis (Table 3). Importantly, tranilast could help commercialized nanomedicine Doxil induce potent cytotoxic effects towards metastatic cancer cells and stimulate antitumor immunity. Finally, the judicious combination of a tranilast, Doxil and ICB cocktail (including PD-1 antibody and cytotoxic T-lymphocyte-associated protein 4, CTLA-4 antibody) achieved synergistic effects in TNBC 4T1 and E0771 tumors, which are notoriously refractory to ICB immunotherapy. The antifibrotic drug tranilast mentioned above, owing to a narrow therapeutic window, may cause adverse effects.[132] To solve this issue, Stylianopoulos *et al.* have leveraged a PEG-*b*-poly (benzyl-L-glutamate) micelle for delivery of tranilast and epirubicin.[175] Notably, tranilast-micelles loaded with one percent of free drug dosage still exhibited superior effects than free drug, in maintaining drug plasma concentration and bioavailability, facilitating CAF drug uptake and hindering the TGF-β signaling pathway in CAFs. Daily administration of tranilast-micelles achieved the optimum effect in reducing IFP and elastic modulus (Table 3). As a result, tranilast-micelles restored intratumoral blood perfusion and enhanced the tumor accumulation and antitumor efficacy of epirubicin-micelles. Furthermore, the synergistic application of tranilast-micelles in conjunction with epirubicin-micelles or Doxil and ICB cocktail elicited a remarkable upsurge in T-cell infiltration, thereby engendering a curative response and enduring immunological memory in murine models of immunotherapy-resistant breast cancers.[175] Of particular note, shear wave elastography (SWE) was used to detect the change of tumor elastic modulus during the course of treatments and a linear correlation between tumor stiffness and antitumor efficacy was established, rendering tumor stiffness a potential mechanical biomarker for predicting therapeutic effects and responses to ICB immunotherapies.[176] While these studies revealed the impacts of tranilast or tranilast-micelles on the TMME, their effects on the tumor immune microenvironment and the mechanism by which TMME normalization affects effector CD8$^+$ T cells still need further investigations.

Matrix metalloproteinases (MMPs) that are highly expressed by macrophages have also been used to mediate the TMME. An elegant study was performed by Yang *et al.*, who prepared metformin-loaded mannose-modified macrophage-derived microparticles (Met@Man-MPs) to specifically target M2 TAMs and repolarize them to M1 phenotype.[177] It was demonstrated that Met@Man-MP-mediated reeducation of TAMs remodeled the tumor immune microenvironment by promoting the infiltration of effector CD8$^+$ T cells into tumor parenchyma and

inhibiting the recruitment of immunosuppressive immune cells, such as myeloid-derived suppressor cells and regulatory T cells. By degrading collagen to increase the infiltration of effector CD8$^+$ T cells and tumor accumulation of PD-1 antibody, the MMPs (including MMP9 and MMP14 proteins) on the surfaces of Met@Man-MPs further amplified the antitumor immunity (Table 3). As a consequence, Met@Man-MPs and PD-1 antibody collectively induced robust and long-lasting antitumor immune effects not only in rodent tumor models but also in organotypic slices of HCC patient-derived tumor. However, the effects of Met@Man-MPs on tumor mechanical properties, including mechanical stiffness, solid stress and IFP, remain to be studied in the future.

Concluding remarks

Regulating tumor mechanical properties with nanomedicine for augmented cancer therapy is at an initial stage of comprehension. Although some progress has been made, as summarized in Fig. 2 and Table 3, there are numerous fundamental challenges and opportunities ahead.

First, a risk of promoting cancer progression exists in regulating the TMME for cancer therapy. Although losartan in combination with FOLFIRINOX and chemoradiotherapy has achieved success for patients with locally advanced pancreatic cancers in a phase II clinical trial,[130] mixed clinical outcomes were observed in PEGPH20 for PDAC patients in phase II and phase III trials.[137,138] Therefore, this risk cannot be ignored. While tumor tissues are usually stiff, cancer cells derived from patients and mice are soft.[61,68] Highly tumorigenic CSC-like tumor repopulating cells, as selected and enriched by 3D soft fibrin gels, are even softer relative to conventional cancer cells.[178] Cancer cells adopt their mechanical properties for invasion and metastasis.[179,180] Therefore, a holistic approach should be undertaken in regulating tumor mechanics for enhanced cancer therapy. One unique advantage of nanomedicines is that nanocarriers can simultaneously deliver two or more antitumor drugs with different mechanisms of action. As such, encapsulating two active ingredients, one for regulating the TMME and the other for eliminating cancer cells, within single nanocarrier holds significant promise for cancer therapy.[181]

Second, of the eight classes of nanomedicines (Doxil, epirubicin-micelles, tranilast-micelles, Met@Man-MPs, FDINs, CHI, mP, and UNPSs) discussed above, Doxil has been applied in the clinic for more than thirty years. The antitumor efficacy of repurposing Doxil for metronomic therapy still needs to be evaluated in prospective clinical trials. While epirubicin-micelles have been tested in phase I/II clinical trial (NCT03168061) and tranilast has been prescribed for patients in the clinic, the clinical translation of tranilast-micelles faces numerous obstacles. Establishing the standards for tranilast-micelle constitution and content, tranilast-micelle size distribution, mean diameter and long-term stability, and drug encapsulation efficiency and loading content in a Good

Manufacturing Practice of Medical Products (GMP) production department is essential. Although tumor cell-derived microparticles (MPs) have achieved successes in lung cancer patients with metastatic malignant pleural effusion (MPE) and in patients with obstructive extrahepatic cholangiocarcinoma[182,183] and been applied clinically in eight provinces or municipalities of China, Met@Man-MPs have not been evaluated in clinical settings. Indeed, replacing cell resources for MP fabrication is a big issue. Therefore, Met@Man-MPs are at an initial stage of clinical translation. HES is a semisynthetic polysaccharide, exhibits good manufacture practice, biocompatibility and biodegradability, and has been used as a clinical plasma substitute for more than fifty years.[184] However, chemical reactions have been performed on HES to obtain HES-based smart nanomedicines, such as FDINs and CHI. Therefore, the clinical translations of FDINs and CHI are also at an initial stage. Numerous challenges, including scale-up of production, quality control, and regulations, lie ahead. From a translational perspective, Doxil, epirubicin-micelles, tranilast-micelles, Met@Man-MPs, FDINs, and CHI have advantages over mesoporous polydopamine (mP) and upconversion nanophotosensitizers (UNPSs) in terms of biocompatibility and biodegradability.

Third, the interplay among solid stress, mechanical stiffness and IFP remains to be studied. While cancer cells, CAFs and ECM components are recognized as the origins of the abnormal mechanical properties, the key determinants for accumulated solid stress, enhanced mechanical stiffness and elevated interstitial fluid pressure are largely unknown. In some previous studies,[37–39,132,175,177] the changes in collagen I, fibronectin and HA have been documented. Such variations have been used to account for the reduction of solid stress, mechanical stiffness and IFP. However, these studies fail to delve into the underlying mechanisms. While collagen fibers are identified to resist tensile loads and HA mainly withstands compression,[8] their contributions in solid stress, mechanical stiffness and IFP are unclear. Numerous hydrogel microspheres have been prepared to probe the forces and stress fields generated by cells within 3D ECM.[185–188] In one seminal study, a hydrogel microsphere-based magnetic microrobot was designed to quantify both forces and stiffness of tumor colonies.[189] Although these hydrogel-based microspheres are promising, they are difficult to use for characterizing aberrant mechanical properties in tumor tissues *in vivo*. Nanoparticles are well known for easy modification and versatile functionalities. It would be interesting to prepare theranostic nanomedicines that are capable of modulating and quantifying the TMME at the same time in tumor tissues. Constructing such multifunctional theranostic nanomedicines will not only help delineate the abnormal tumor mechanical microenvironment, but more importantly will yield efficient cancer therapy.

Conflicts of interest

There are no conflicts to declare.

Acknowledgements

References

1 H. T. Nia, L. L. Munn and R. K. Jain, *Science*, 2020, **370**, eaaz086.

2 W. A. Berg, D. O. Cosgrove, C. J. Dore, F. K. Schafer, W. E. Svensson, R. J. Hooley, R. Ohlinger, E. B. Mendelson, C. Balu-Maestro, M. Locatelli, C. Tourasse, B. C. Cavanaugh, V. Juhan, A. T. Stavros, A. Tardivon, J. Gay, J. P. Henry, C. Cohen-Bacrie and B. E. Investigators, *Radiology*, 2012, **262**, 435–449.

3 R. Masuzaki, R. Tateishi, H. Yoshida, E. Goto, T. Sato, T. Ohki, J. Imamura, T. Goto, F. Kanai, N. Kato, H. Ikeda, S. Shiina, T. Kawabe and M. Omata, *Hepatology*, 2009, **49**, 1954–1961.

4 J. Iglesias-Garcia, J. Larino-Noia, I. Abdulkader, J. Forteza and J. E. Dominguez-Munoz, *Gastroenterology*, 2010, **139**, 1172–1180.

5 T. J. Kirby and J. Lammerding, *Nat. Cell Biol.*, 2018, **20**, 373–381.

6 K. R. Leventhal, H. Yu, L. Kass, J. N. Lakins, M. Egeblad, J. T. Erler, S. F. Fong, K. Csiszar, A. Giaccia, W. Weninger, M. Yamauchi, D. L. Gasser and V. M. Weaver, *Cell*, 2009, **139**, 891–906.

7 T. Lecuit and A. S. Yap, *Nat. Cell Biol.*, 2015, **17**, 533–539.

8 T. Stylianopoulos, L. L. Munn and R. K. Jain, *Trends Cancer*, 2018, **4**, 292–319.

9 M. J. Mitchell, R. K. Jain and R. Langer, *Nat. Rev. Cancer*, 2017, **17**, 659–675.

10 R. K. Jain, J. D. Martin and T. Stylianopoulos, *Annu. Rev. Biomed. Eng.*, 2014, **16**, 321–346.

11 M. C. Lampi and C. A. Reinhart-King, *Sci. Transl. Med.*, 2018, **10**, eaao0475.

12 V. Barry-Hamilton, R. Spangler, D. Marshall, S. McCauley, H. M. Rodriguez, M. Oyasu, A. Mikels, M. Vaysberg, H. Ghermazien, C. Wai, C. A. Garcia, A. C. Velayo, B. Jorgensen, D. Biermann, D. Tsai, J. Green, S. Zaffryar-Eilot, A. Holzer, S. Ogg, D. Thai, G. Neufeld, P. Van Vlasselaer and V. Smith, *Nat. Med.*, 2010, **16**, 1009–1017.

13 J. Liu, S. Liao, B. Diop-Frimpong, W. Chen, S. Goel, K. Naxerova, M. Ancukiewicz, Y. Boucher, R. K. Jain and

L. Xu, *Proc. Natl. Acad. Sci. U. S. A.*, 2012, **109**, 16618–16623.

14 P. P. Provenzano, C. Cuevas, A. E. Chang, V. K. Goel, D. D. Von Hoff and S. R. Hingorani, *Cancer Cell*, 2012, **21**, 418–429.

15 I. X. Chen, V. P. Chauhan, J. Posada, M. R. Ng, M. W. Wu, P. Adstamongkonkul, P. Huang, N. Lindeman, R. Langer and R. K. Jain, *Proc. Natl. Acad. Sci. U. S. A.*, 2019, **116**, 4558–4566.

16 J. Shi, P. W. Kantoff, R. Wooster and O. C. Farokhzad, *Nat. Rev. Cancer*, 2017, **17**, 20–37.

17 S. Li, Y. Zhang, J. Wang, Y. Zhao, T. Ji, X. Zhao, Y. Ding, X. Zhao, R. Zhao, F. Li, X. Yang, S. Liu, Z. Liu, J. Lai, A. K. Whittaker, G. J. Anderson, J. Wei and G. Nie, *Nat. Biomed. Eng.*, 2017, **1**, 667–679.

18 H. B. Chen, Z. J. Gu, H. W. An, C. Y. Chen, J. Chen, R. Cui, S. Q. Chen, W. H. Chen, X. S. Chen, X. Y. Chen, Z. Chen, B. Q. Ding, Q. Dong, Q. Fan, T. Fu, D. Y. Hou, Q. Jiang, H. T. Ke, X. Q. Jiang, G. Liu, S. P. Li, T. Y. Li, Z. Liu, G. J. Nie, M. Ovais, D. W. Pang, N. S. Qiu, Y. Q. Shen, H. Y. Tian, C. Wang, H. Wang, Z. Q. Wang, H. P. Xu, J. F. Xu, X. L. Yang, S. Zhu, X. C. Zheng, X. Z. Zhang, Y. B. Zhao, W. H. Tan, X. Zhang and Y. L. Zhao, *Sci. China: Chem.*, 2018, **61**, 1503–1552.

19 R. K. Jain and T. Stylianopoulos, *Nat. Rev. Clin Oncol.*, 2010, **7**, 653–664.

20 V. P. Chauhan and R. K. Jain, *Nat. Mater.*, 2013, **12**, 958–962.

21 W. Deng, W. Chen, S. Clement, A. Guller, Z. Zhao, A. Engel and E. M. Goldys, *Nat. Commun.*, 2018, **9**, 2713.

22 N. Ma, H. Xu, L. An, J. Li, Z. Sun and X. Zhang, *Langmuir*, 2011, **27**, 5874–5878.

23 R. J. Passarella, D. E. Spratt, A. E. van der Ende, J. G. Phillips, H. Wu, V. Sathiyakumar, L. Zhou, D. E. Hallahan, E. Harth and R. Diaz, *Cancer Res.*, 2010, **70**, 4550–4559.

24 X. Yi, L. Chen, J. Chen, D. Maiti, Z. F. Chai, Z. Liu and K. Yang, *Adv. Funct. Mater.*, 2018, **28**, 1705161.

25 G. Erel-Akbaba, L. A. Carvalho, T. Tian, M. Zinter, H. Akbaba, P. J. Obeid, E. A. Chiocca, R. Weissleder, A. G. Kantarci and B. A. Tannous, *ACS Nano*, 2019, **13**, 4028–4040.

26 Key reference: X. Wu, Y. Zhu, W. Huang, J. Li, B. Zhang, Z. Li and X. Yang, *Adv. Sci.*, 2018, **5**, 1700859.

27 Key reference: X. Liu, N. B. Ye, C. Xiao, X. X. Wang, S. Y. Li, Y. H. Deng, X. Q. Yang, Z. F. Li and X. L. Yang, *Nano Today*, 2021, **40**, 101248.

28 J. Li, J. Huang, Y. Ao, S. Li, Y. Miao, Z. Yu, L. Zhu, X. Lan, Y. Zhu, Y. Zhang and X. Yang, *ACS Appl. Mater. Interfaces*, 2018, **10**, 22985–22996.

29 Key reference: X. Liu, N. Ye, S. Liu, J. Guan, Q. Deng, Z. Zhang, C. Xiao, Z. Y. Ding, B. X. Zhang, X. P. Chen, Z. Li and X. Yang, *Adv. Sci.*, 2021, **8**, e2100233.

30 Key reference: X. X. Wang, N. B. Ye, C. Xu, C. Xiao, Z. J. Zhang, Q. Y. Deng, S. Y. Li, J. Y. Li, Z. F. Li and X. L. Yang, *Nano Today*, 2022, **44**, 101458.

31 Key reference: J. Chen, Z. Zhang, Y. Li, H. Zeng, Z. Li, C. Wang, C. Xu, Q. Deng, Q. Wang, X. Yang and Z. Li, *J. Mater. Chem. B*, 2022, **10**, 8193–8210.

32 A. R. Kirtane, T. Sadhukha, H. Kim, V. Khanna, B. Koniar and J. Panyam, *Cancer Res.*, 2017, **77**, 1465–1475.

33 B. Zhang, T. Jiang, X. She, S. Shen, S. Wang, J. Deng, W. Shi, H. Mei, Y. Hu, Z. Pang and X. Jiang, *Biomaterials*, 2016, **96**, 63–71.

34 J. W. Snyder, W. R. Greco, D. A. Bellnier, L. Vaughan and B. W. Henderson, *Cancer Res.*, 2003, **63**, 8126–8131.

35 H. C. Huang, I. Rizvi, J. Liu, S. Anbil, A. Kalra, H. Lee, Y. Baglo, N. Paz, D. Hayden, S. Pereira, B. W. Pogue, J. Fitzgerald and T. Hasan, *Cancer Res.*, 2018, **78**, 558–571.

36 M. Overchuk, K. M. Harmatys, S. Sindhwani, M. A. Rajora, A. Koebel, D. M. Charron, A. M. Syed, J. Chen, M. G. Pomper, B. C. Wilson, W. C. W. Chan and G. Zheng, *Nano Lett.*, 2021, **21**, 344–352.

37 Key reference: C. Wang, H. M. Wang, H. Yang, C. Xu, Q. Wang, Z. Li, Z. J. Zhang, J. K. Guan, X. M. Yu, X. Q. Yang, X. L. Yang and Z. F. Li, *Nano Res.*, 2023, **16**, 7323–7336.

38 Key reference: C. Wang, Q. Wang, H. Wang, Z. Li, J. Chen, Z. Zhang, H. Zeng, X. Yu, X. Yang, X. Yang and Z. Li, *J. Controlled Release*, 2023, **353**, 391–410.

39 Key reference: Y. X. Xiong, W. Wang, Q. Y. Deng, Z. J. Zhang, Q. Wang, Z. T. Yong, C. Y. Sun, X. L. Yang and Z. F. Li, *Nano Today*, 2023, **49**, 101767.

40 Key reference: Z. Zhang, Z. Wang, Y. Xiong, C. Wang, Q. Deng, T. Yang, Q. Xu, Z. Yong, X. Yang and Z. Li, *Biomater. Sci.*, 2022, **11**, 108–118.

41 T. Tan, H. Hu, H. Wang, J. Li, Z. Wang, J. Wang, S. Wang, Z. Zhang and Y. Li, *Nat. Commun.*, 2019, **10**, 3322.

42 Y. Wang, H. Xie, Y. Wu, S. Xu, Y. Li, J. Li, X. Xu, S. Wang, Y. Li and Z. Zhang, *Adv. Mater.*, 2022, **34**, e2110614.

43 J. Kolosnjaj-Tabi, R. Di Corato, L. Lartigue, I. Marangon, P. Guardia, A. K. Silva, N. Luciani, O. Clement, P. Flaud, J. V. Singh, P. Decuzzi, T. Pellegrino, C. Wilhelm and F. Gazeau, *ACS Nano*, 2014, **8**, 4268–4283.

44 A. Nicolas-Boluda, J. Vaquero, G. Laurent, G. Renault, R. Bazzi, E. Donnadieu, S. Roux, L. Fouassier and F. Gazeau, *ACS Nano*, 2020, **14**, 5738–5753.

45 I. Marangon, A. A. Silva, T. Guilbert, J. Kolosnjaj-Tabi, C. Marchiol, S. Natkhunarajah, F. Chamming's, C. Menard-Moyon, A. Bianco, J. L. Gennisson, G. Renault and F. Gazeau, *Theranostics*, 2017, **7**, 329–343.

46 J. Kolosnjaj-Tabi, I. Marangon, A. Nicolas-Boluda, A. K. A. Silva and F. Gazeau, *Pharmacol. Res.*, 2017, **126**, 123–137.

47 A. Nicolas-Boluda, A. K. A. Silva, S. Fournel and F. Gazeau, *Biomaterials*, 2018, **150**, 87–99.

48 X. Han, Y. Xu, M. Geranpayehvaghei, G. J. Anderson, Y. Li and G. Nie, *Biomaterials*, 2020, **232**, 119745.

49 J. J. Liu, Q. Chen, L. Z. Feng and Z. Liu, *Nano Today*, 2018, **21**, 55–73.

50 D. Zhang, G. Wang, X. Yu, T. Wei, L. Farbiak, L. T. Johnson, A. M. Taylor, J. Xu, Y. Hong, H. Zhu and D. J. Siegwart, *Nat. Nanotechnol.*, 2022, **17**, 777–787.

51 Y. Zhong, J. Zhang, J. Zhang, Y. Hou, E. Chen, D. Huang, W. Chen and R. Haag, *Adv. Funct. Mater.*, 2021, **31**, 2007544.

52 Y. Jiang, H. Zhang, J. Wang, Y. Liu, T. Luo and H. Hua, *J. Hematol. Oncol.*, 2022, **15**, 34.

53 H. T. Nia, H. Liu, G. Seano, M. Datta, D. Jones, N. Rahbari, J. Incio, V. P. Chauhan, K. Jung, J. D. Martin, V. Askoxylakis, T. P. Padera, D. Fukumura, Y. Boucher, F. J. Hornicek, A. J. Grodzinsky, J. W. Baish, L. L. Munn and R. K. Jain, *Nat. Biomed. Eng.*, 2016, **1**, 0004.

54 J. D. Martin, G. Seano and R. K. Jain, *Annu. Rev. Physiol.*, 2019, **81**, 505–534.

55 V. Panzetta, I. Musella, I. Rapa, M. Volante, P. A. Netti and S. Fusco, *Acta Biomater.*, 2017, **57**, 334–341.

56 N. F. Boyd, Q. Li, O. Melnichouk, E. Huszti, L. J. Martin, A. Gunasekara, G. Mawdsley, M. J. Yaffe and S. Minkin, *PLoS One*, 2014, **9**, e100937.

57 R. K. Jain, *Cancer Cell*, 2014, **26**, 605–622.

58 T. Stylianopoulos, J. D. Martin, V. P. Chauhan, S. R. Jain, B. Diop-Frimpong, N. Bardeesy, B. L. Smith, C. R. Ferrone, F. J. Hornicek, Y. Boucher, L. L. Munn and R. K. Jain, *Proc. Natl. Acad. Sci. U. S. A.*, 2012, **109**, 15101–15108.

59 V. P. Chauhan, J. D. Martin, H. Liu, D. A. Lacorre, S. R. Jain, S. V. Kozin, T. Stylianopoulos, A. S. Mousa, X. Han, P. Adstamongkonkul, Z. Popovic, P. Huang, M. G. Bawendi, Y. Boucher and R. K. Jain, *Nat. Commun.*, 2013, **4**, 2516.

60 T. Stylianopoulos, J. D. Martin, M. Snuderl, F. Mpekris, S. R. Jain and R. K. Jain, *Cancer Res.*, 2013, **73**, 3833–3841.

61 M. Plodinec, M. Loparic, C. A. Monnier, E. C. Obermann, R. Zanetti-Dallenbach, P. Oertle, J. T. Hyotyla, U. Aebi, M. Bentires-Alj, R. Y. Lim and C. A. Schoenenberger, *Nat. Nanotechnol.*, 2012, **7**, 757–765.

62 M. Tian, Y. Li, W. Liu, L. Jin, X. Jiang, X. Wang, Z. Ding, Y. Peng, J. Zhou, J. Fan, Y. Cao, W. Wang and Y. Shi, *Nanoscale*, 2015, **7**, 12998–13010.

63 M. Lekka, D. Gil, K. Pogoda, J. Dulinska-Litewka, R. Jach, J. Gostek, O. Klymenko, S. Prauzner-Bechcicki, Z. Stachura, J. Wiltowska-Zuber, K. Okon and P. Laidler, *Arch. Biochem. Biophys.*, 2012, **518**, 151–156.

64 G. Ciasca, T. E. Sassun, E. Minelli, M. Antonelli, M. Papi, A. Santoro, F. Giangaspero, R. Delfini and M. De Spirito, *Nanoscale*, 2016, **8**, 19629–19643.

65 S. E. Cross, Y. S. Jin, J. Rao and J. K. Gimzewski, *Nat. Nanotechnol.*, 2007, **2**, 780–783.

66 S. Suresh, *Acta Biomater.*, 2007, **3**, 413–438.

67 J. Chung, Y. J. Kim and E. Yoon, *Appl. Phys. Lett.*, 2011, **98**, 123701.

68 T. Fuhs, F. Wetzel, A. W. Fritsch, X. Z. Li, R. Stange, S. Pawlizak, T. R. Kiessling, E. Morawetz, S. Grosser, F. Sauer, J. Lippoldt, F. Renner, S. Friebe, M. Zink, K. Bendrat, J. Braun, M. H. Oktay, J. Condeelis, S. Briest, B. Wolf, L. C. Horn, M. Hockel, B. Aktas, M. C. Marchetti, M. L. Manning, A. Niendorf, D. P. Bi and J. A. Kas, *Nat. Phys.*, 2022, **18**, 1510–1519.

69 E. Sahai, I. Astsaturov, E. Cukierman, D. G. DeNardo, M. Egeblad, R. M. Evans, D. Fearon, F. R. Greten, S. R. Hingorani, T. Hunter, R. O. Hynes, R. K. Jain, T. Janowitz, C. Jorgensen, A. C. Kimmelman, M. G. Kolonin, R. G. Maki, R. S. Powers, E. Pure, D. C. Ramirez, R. Scherz-Shouval, M. H. Sherman, S. Stewart, T. D. Tlsty, D. A. Tuveson, F. M. Watt, V. Weaver, A. T. Weeraratna and Z. Werb, *Nat. Rev. Cancer*, 2020, **20**, 174–186.

70 J. Lee, S. Condello, B. Yakubov, R. Emerson, A. Caperell-Grant, K. Hitomi, J. Xie and D. Matei, *Clin. Cancer Res.*, 2015, **21**, 4482–4493.

71 C. Storm, J. J. Pastore, F. C. MacKintosh, T. C. Lubensky and P. A. Janmey, *Nature*, 2005, **435**, 191–194.

72 G. Seano, H. T. Nia, K. E. Emblem, M. Datta, J. Ren, S. Krishnan, J. Kloepper, M. C. Pinho, W. W. Ho, M. Ghosh, V. Askoxylakis, G. B. Ferraro, L. Riedemann, E. R. Gerstner, T. T. Batchelor, P. Y. Wen, N. U. Lin, A. J. Grodzinsky, D. Fukumura, P. Huang, J. W. Baish, T. P. Padera, L. L. Munn and R. K. Jain, *Nat. Biomed. Eng.*, 2019, **3**, 230–245.

73 D. Choquet, D. P. Felsenfeld and M. P. Sheetz, *Cell*, 1997, **88**, 39–48.

74 J. Liang, J. Ampuero, J. Castell, Q. Zhang, S. Zhang, Y. Chen and M. Romero-Gomez, *Ann. Hepatol.*, 2022, **28**, 100889.

75 Y. K. Mariappan, K. J. Glaser and R. L. Ehman, *Clin. Anat.*, 2010, **23**, 497–511.

76 K. J. Parker, M. M. Doyley and D. J. Rubens, *Phys. Med. Biol.*, 2011, **56**, R1–R29.

77 V. Ajmera, B. K. Kim, K. Yang, A. M. Majzoub, T. Nayfeh, N. Tamaki, N. Izumi, A. Nakajima, R. Idilman, M. Gumussoy, D. K. Oz, A. Erden, N. E. Quach, X. Tu, X. Zhang, M. Noureddin, A. M. Allen and R. Loomba, *Gastroenterology*, 2022, **163**, 1079–1089.

78 D. B. Plewes, I. Betty, S. N. Urchuk and I. Soutar, *J. Magn. Reson. Imaging*, 1995, **5**, 733–738.

79 R. Muthupillai, D. J. Lomas, P. J. Rossman, J. F. Greenleaf, A. Manduca and R. L. Ehman, *Science*, 1995, **269**, 1854–1857.

80 A. Itoh, E. Ueno, E. Tohno, H. Kamma, H. Takahashi, T. Shiina, M. Yamakawa and T. Matsumura, *Radiology*, 2006, **239**, 341–350.

81 R. G. Barr, G. Ferraioli, M. L. Palmeri, Z. D. Goodman, G. Garcia-Tsao, J. Rubin, B. Garra, R. P. Myers, S. R. Wilson, D. Rubens and D. Levine, *Radiology*, 2015, **276**, 845–861.

82 G. Ferraioli, C. Filice, L. Castera, B. I. Choi, I. Sporea, S. R. Wilson, D. Cosgrove, C. F. Dietrich, D. Amy, J. C. Bamber, R. Barr, Y. H. Chou, H. Ding, A. Farrokh, M. Friedrich-Rust, T. J. Hall, K. Nakashima, K. R. Nightingale, M. L. Palmeri, F. Schafer, T. Shiina, S. Suzuki and M. Kudo, *Ultrasound Med. Biol.*, 2015, **41**, 1161–1179.

83 Q. Luo, D. Kuang, B. Zhang and G. Song, *Biochim. Biophys. Acta*, 2016, **1860**, 1953–1960.

84 A. Stylianou, M. Lekka and T. Stylianopoulos, *Nanoscale*, 2018, **10**, 20930–20945.

85 M. Krieg, G. Flaschner, D. Alsteens, B. M. Gaub, W. H. Roos, G. J. L. Wuite, H. E. Gaub, C. Gerber, Y. F. Dufrene and D. J. Muller, *Nat. Rev. Phys.*, 2019, **1**, 41–57.

86 C. Voutouri, C. Polydorou, P. Papageorgis, V. Gkretsi and T. Stylianopoulos, *Neoplasia*, 2016, **18**, 732–741.

87 M. Panagi, C. Voutouri, F. Mpekris, P. Papageorgis, M. R. Martin, J. D. Martin, P. Demetriou, C. Pierides, C. Polydorou, A. Stylianou, M. Louca, L. Koumas, P. Costeas, K. Kataoka, H. Cabral and T. Stylianopoulos, *Theranostics*, 2020, **10**, 1910–1922.

88 M. J. Paszek, N. Zahir, K. R. Johnson, J. N. Lakins, G. I. Rozenberg, A. Gefen, C. A. Reinhart-King, S. S. Margulies, M. Dembo, D. Boettiger, D. A. Hammer and V. M. Weaver, *Cancer Cell*, 2005, **8**, 241–254.

89 X. Tang, T. B. Kuhlenschmidt, Q. Li, S. Ali, S. Lezmi, H. Chen, M. Pires-Alves, W. W. Laegreid, T. A. Saif and M. S. Kuhlenschmidt, *Mol. Cancer*, 2014, **13**, 131.

90 X. Tang, T. B. Kuhlenschmidt, J. Zhou, P. Bell, F. Wang, M. S. Kuhlenschmidt and T. A. Saif, *Biophys. J.*, 2010, **99**, 2460–2469.

91 S. C. Wei, L. Fattet, J. H. Tsai, Y. Guo, V. H. Pai, H. E. Majeski, A. C. Chen, R. L. Sah, S. S. Taylor, A. J. Engler and J. Yang, *Nat. Cell Biol.*, 2015, **17**, 678–688.

92 I. Acerbi, L. Cassereau, I. Dean, Q. Shi, A. Au, C. Park, Y. Y. Chen, J. Liphardt, E. S. Hwang and V. M. Weaver, *Integr. Biol.*, 2015, **7**, 1120–1134.

93 R. S. Goertz, J. Schuderer, D. Strobel, L. Pfeifer, M. F. Neurath and D. Wildner, *Eur. J. Radiol.*, 2016, **85**, 2211–2216.

94 A. J. Rice, E. Cortes, D. Lachowski, B. C. H. Cheung, S. A. Karim, J. P. Morton and A. Del Rio Hernandez, *Oncogenesis*, 2017, **6**, e352.

95 F. J. Sulzmaier, C. Jean and D. D. Schlaepfer, *Nat. Rev. Cancer*, 2014, **14**, 598–610.

96 F. Calvo, N. Ege, A. Grande-Garcia, S. Hooper, R. P. Jenkins, S. I. Chaudhry, K. Harrington, P. Williamson, E. Moeendarbary, G. Charras and E. Sahai, *Nat. Cell Biol.*, 2013, **15**, 637–646.

97 S. Dupont, L. Morsut, M. Aragona, E. Enzo, S. Giulitti, M. Cordenonsi, F. Zanconato, J. Le Digabel, M. Forcato, S. Bicciato, N. Elvassore and S. Piccolo, *Nature*, 2011, **474**, 179–183.

98 J. Xu, S. Lamouille and R. Derynck, *Cell Res.*, 2009, **19**, 156–172.

99 G. Helmlinger, P. A. Netti, H. C. Lichtenbeld, R. J. Melder and R. K. Jain, *Nat. Biotechnol.*, 1997, **15**, 778–783.

100 C. P. Heisenberg and Y. Bellaiche, *Cell*, 2013, **153**, 948–962.

101 K. D. Irvine and B. I. Shraiman, *Development*, 2017, **144**, 4238–4248.

102 C. Fernandez Moro, B. Bozoky and M. Gerling, *BMJ Open Gastroenterol.*, 2018, **5**, e000217.

103 D. D. Simon, C. O. Horgan and J. D. Humphrey, *J. Mech. Behav. Biomed. Mater.*, 2012, **14**, 216–226.

104 G. Cheng, J. Tse, R. K. Jain and L. L. Munn, *PLoS One*, 2009, **4**, e4632.

105 H. T. Nia, M. Datta, G. Seano, P. Huang, L. L. Munn and R. K. Jain, *Nat. Protoc.*, 2018, **13**, 1091–1105.

106 T. P. Padera, B. R. Stoll, J. B. Tooredman, D. Capen, E. di Tomaso and R. K. Jain, *Nature*, 2004, **427**, 695.

107 G. Griffon-Etienne, Y. Boucher, C. Brekken, H. D. Suit and R. K. Jain, *Cancer Res.*, 1999, **59**, 3776–3782.

108 B. W. Benham-Pyle, B. L. Pruitt and W. J. Nelson, *Science*, 2015, **348**, 1024–1027.

109 B. Coste, J. Mathur, M. Schmidt, T. J. Earley, S. Ranade, M. J. Petrus, A. E. Dubin and A. Patapoutian, *Science*, 2010, **330**, 55–60.

110 A. Elosegui-Artola, I. Andreu, A. E. M. Beedle, A. Lezamiz, M. Uroz, A. J. Kosmalska, R. Oria, J. Z. Kechagia, P. Rico-Lastres, A. L. Le Roux, C. M. Shanahan, X. Trepat, D. Navajas, S. Garcia-Manyes and P. Roca-Cusachs, *Cell*, 2017, **171**, 1397–1410.

111 F. Zanconato, M. Cordenonsi and S. Piccolo, *Cancer Cell*, 2016, **29**, 783–803.

112 M. L. Smith, D. Gourdon, W. C. Little, K. E. Kubow, R. A. Eguiluz, S. Luna-Morris and V. Vogel, *PLoS Biol.*, 2007, **5**, e268.

113 K. Saini, S. Cho, L. J. Dooling and D. E. Discher, *Matrix Biol.*, 2020, **85–86**, 34–46.

114 K. E. Kubow, R. Vukmirovic, L. Zhe, E. Klotzsch, M. L. Smith, D. Gourdon, S. Luna and V. Vogel, *Nat. Commun.*, 2015, **6**, 8026.

115 J. S. Young, C. E. Lumsden and A. L. Stalker, *J. Pathol. Bacteriol.*, 1950, **62**, 313–333.

116 H. O. Fadnes, R. K. Reed and K. Aukland, *Microvasc. Res.*, 1977, **14**, 27–36.

117 Y. Boucher, L. T. Baxter and R. K. Jain, *Cancer Res.*, 1990, **50**, 4478–4484.

118 M. A. Swartz and A. W. Lund, *Nat. Rev. Cancer*, 2012, **12**, 210–219.

119 J. W. Song and L. L. Munn, *Proc. Natl. Acad. Sci. U. S. A.*, 2011, **108**, 15342–15347.

120 H. Qazi, Z. D. Shi and J. M. Tarbell, *PLoS One*, 2011, **6**, e20348.

121 W. J. Polacheck, J. L. Charest and R. D. Kamm, *Proc. Natl. Acad. Sci. U. S. A.*, 2011, **108**, 11115–11120.

122 S. F. Chang, C. A. Chang, D. Y. Lee, P. L. Lee, Y. M. Yeh, C. R. Yeh, C. K. Cheng, S. Chien and J. J. Chiu, *Proc. Natl. Acad. Sci. U. S. A.*, 2008, **105**, 3927–3932.

123 D. E. Leckband and J. de Rooij, *Annu. Rev. Cell Dev. Biol.*, 2014, **30**, 291–315.

124 W. J. Polacheck, M. L. Kutys, J. Yang, J. Eyckmans, Y. Wu, H. Vasavada, K. K. Hirschi and C. S. Chen, *Nature*, 2017, **552**, 258–262.

125 K. C. Wang, Y. T. Yeh, P. Nguyen, E. Limqueco, J. Lopez, S. Thorossian, K. L. Guan, Y. J. Li and S. Chien, *Proc. Natl. Acad. Sci. U. S. A.*, 2016, **113**, 11525–11530.

126 L. Wang, J. Y. Luo, B. Li, X. Y. Tian, L. J. Chen, Y. Huang, J. Liu, D. Deng, C. W. Lau, S. Wan, D. Ai, K. K. Mak, K. K. Tong, K. M. Kwan, N. Wang, J. J. Chiu, Y. Zhu and Y. Huang, *Nature*, 2016, **540**, 579–582.

127 A. Zinger, L. Koren, O. Adir, M. Poley, M. Alyan, Z. Yaari, N. Noor, N. Krinsky, A. Simon, H. Gibori, M. Krayem, Y. Mumblat, S. Kasten, S. Ofir, E. Fridman, N. Milman, M. M. Lubtow, L. Liba, J. Shklover, J. Shainsky-Roitman, Y. Binenbaum, D. Hershkovitz, Z. Gil, T. Dvir, R. Luxenhofer, R. Satchi-Fainaro and A. Schroeder, *ACS Nano*, 2019, **13**, 11008–11021.

128 K. Hama, H. Ohnishi, H. Yasuda, N. Ueda, H. Mashima, Y. Satoh, K. Hanatsuka, H. Kita, A. Ohashi, K. Tamada and K. Sugano, *Biochem. Biophys. Res. Commun.*, 2004, **315**, 905–911.

129 W. B. Liu, X. P. Wang, K. Wu and R. L. Zhang, *World J. Gastroenterol.*, 2005, **11**, 6489–6494.

130 J. E. Murphy, J. Y. Wo, D. P. Ryan, J. W. Clark, W. Jiang, B. Y. Yeap, L. C. Drapek, L. Ly, C. V. Baglini, L. S. Blaszkowsky, C. R. Ferrone, A. R. Parikh, C. D. Weekes, R. D. Nipp, E. L. Kwak, J. N. Allen, R. B. Corcoran, D. T. Ting, J. E. Faris, A. X. Zhu, L. Goyal, D. L. Berger, M. Qadan, K. D. Lillemoe, N. Talele, R. K. Jain, T. F. DeLaney, D. G. Duda, Y. Boucher, C. Fernandez-Del Castillo and T. S. Hong, *JAMA Oncol.*, 2019, **5**, 1020–1027.

131 P. Papageorgis, C. Polydorou, F. Mpekris, C. Voutouri, E. Agathokleous, C. P. Kapnissi-Christodoulou and T. Stylianopoulos, *Sci. Rep.*, 2017, **7**, 46140.

132 F. Mpekris, M. Panagi, C. Voutouri, J. D. Martin, R. Samuel, S. Takahashi, N. Gotohda, T. Suzuki, P. Papageorgis, P. Demetriou, C. Pierides, L. Koumas, P. Costeas, M. Kojima, G. Ishii, A. Constantinidou, K. Kataoka, H. Cabral and T. Stylianopoulos, *Adv. Sci.*, 2021, **8**, 2001917.

133 C. Polydorou, F. Mpekris, P. Papageorgis, C. Voutouri and T. Stylianopoulos, *Oncotarget*, 2017, **8**, 24506–24517.

134 C. Voutouri and T. Stylianopoulos, *PLoS One*, 2018, **13**, e0193801.

135 V. P. Chauhan, Y. Boucher, C. R. Ferrone, S. Roberge, J. D. Martin, T. Stylianopoulos, N. Bardeesy, R. A. DePinho, T. P. Padera, L. L. Munn and R. K. Jain, *Cancer Cell*, 2014, **26**, 14–15.

136 S. R. Hingorani, W. P. Harris, J. T. Beck, B. A. Berdov, S. A. Wagner, E. M. Pshevlotsky, S. A. Tjulandin, O. A. Gladkov, R. F. Holcombe, R. Korn, N. Raghunand, S. Dychter, P. Jiang, H. M. Shepard and C. E. Devoe, *Clin. Cancer Res.*, 2016, **22**, 2848–2854.

137 S. R. Hingorani, L. Zheng, A. J. Bullock, T. E. Seery, W. P. Harris, D. S. Sigal, F. Braiteh, P. S. Ritch, M. M. Zalupski, N. Bahary, P. E. Oberstein, A. Wang-Gillam, W. Wu, D. Chondros, P. Jiang, S. Khelifa, J. Pu, C. Aldrich and A. E. Hendifar, *J. Clin. Oncol.*, 2018, **36**, 359–366.

138 R. K. Ramanathan, S. L. McDonough, P. A. Philip, S. R. Hingorani, J. Lacy, J. S. Kortmansky, J. Thumar, E. G. Chiorean, A. F. Shields, D. Behl, P. T. Mehan, R. Gaur, T. Seery, K. A. Guthrie and H. S. Hochster, *J. Clin. Oncol.*, 2019, **37**, 1062–1069.

139 N. S. Al-Waili, G. J. Butler, J. Beale, R. W. Hamilton, B. Y. Lee and P. Lucas, *Med. Sci. Monit.*, 2005, **11**, RA279–RA289.

140 R. Mayer, M. R. Hamilton-Farrell, A. J. van der Kleij, J. Schmutz, G. Granstrom, Z. Sicko, Y. Melamed, U. M. Carl, K. A. Hartmann, E. C. Jansen, L. Ditri and P. Sminia, *Strahlenther. Onkol.*, 2005, **181**, 113–123.

141 J. Daruwalla and C. Christophi, *World J. Surg.*, 2006, **30**, 2112–2131.

142 H. Bitterman, *Crit. Care*, 2009, **13**, 205.

143 E. Pasquier, M. Kavallaris and N. Andre, *Nat. Rev. Clin Oncol.*, 2010, **7**, 455–465.

144 R. S. Kerbel and B. A. Kamen, *Nat. Rev. Cancer*, 2004, **4**, 423–436.

145 N. Andre, M. Carre and E. Pasquier, *Nat. Rev. Clin Oncol.*, 2014, **11**, 413–431.

146 F. Mpekris, J. W. Baish, T. Stylianopoulos and R. K. Jain, *Proc. Natl. Acad. Sci. U. S. A.*, 2017, **114**, 1994–1999.

147 J. C. Doloff, N. Khan, J. Ma, E. Demidenko, H. M. Swartz and Y. Jounaidi, *Curr. Cancer Drug Targets*, 2009, **9**, 777–788.

148 Key reference: Z. Zhang, Q. Deng, C. Xiao, Z. Li and X. Yang, *Acc. Chem. Res.*, 2022, **55**, 526–536.

149 F. Mpekris, C. Voutouri, M. Panagi, J. W. Baish, R. K. Jain and T. Stylianopoulos, *J. Controlled Release*, 2022, **345**, 190–199.

150 Y. Liu, L. Liu, M. Chen and Q. Zhang, *J. Biomol. Struct. Dyn.*, 2013, **31**, 862–873.

151 M. Dunne, J. C. Evans, M. W. Dewhirst and C. Allen, *Adv. Drug Delivery Rev.*, 2020, **163–164**, 1–2.

152 M. Dunne, M. Regenold and C. Allen, *Adv. Drug Delivery Rev.*, 2020, **163–164**, 98–124.

153 S. Sarkar and N. Levi-Polyachenko, *Adv. Drug Delivery Rev.*, 2020, **163–164**, 40–64.

154 M. Chang, Z. Hou, M. Wang, C. Li and J. Lin, *Adv. Mater.*, 2021, **33**, e2004788.

155 Y. Wan, L. H. Fu, C. Li, J. Lin and P. Huang, *Adv. Mater.*, 2021, **33**, e2103978.

156 L. Ding, Y. Wu, M. Wu, Q. Zhao, H. Li, J. Liu, X. Liu, X. Zhang and Y. Zeng, *ACS Appl. Mater. Interfaces*, 2021, **13**, 52435–52449.

157 Y. Wang, Q. Zhao, B. Zhao, Y. Zheng, Q. Zhuang, N. Liao, P. Wang, Z. Cai, D. Zhang, Y. Zeng and X. Liu, *Adv. Sci.*, 2022, **9**, e2105631.

158 D. Zhang, T. H. Teng, Q. F. Zhao, Z. W. Lin, J. R. Zhang, X. L. Liu and Y. Y. Zeng, *ACS Appl. Nano Mater.*, 2022, **5**, 16741–16752.

159 J. J. Hu, Q. Lei and X. Z. Zhang, *Prog. Mater. Sci.*, 2020, **114**, 100685.

160 I. Jiménez Munguía, I. Meshkov, Y. Gorbunova and V. Sokolov, *Ann. Oncol.*, 2019, **30**, v18.

161 V. A. Ivanova, E. V. Verenikina, V. P. Nikitina, O. E. Zhenilo, P. A. Kruze, I. S. Nikitin and O. I. Kit, *J. Clin. Oncol.*, 2020, **38**, 6035–6035.

162 A. I. Viktoria, P. N. Vera, V. V. Ekaterina, E. Z. Oksana and A. Anna Yu, *J. Clin. Oncol.*, 2022, **40**(16), e17528–e17528.

163 L. Ding, X. Lin, Z. Lin, Y. Wu, X. Liu, J. Liu, M. Wu, X. Zhang and Y. Zeng, *ACS Appl. Mater. Interfaces*, 2020, **12**, 36906–36916.

164 Y. Wu, L. Ding, C. Zheng, H. Li, M. Wu, Y. Sun, X. Liu, X. Zhang and Y. Zeng, *Acta Biomater.*, 2022, **153**, 419–430.

165 S. Lan, Z. Lin, D. Zhang, Y. Zeng and X. Liu, *ACS Appl. Mater. Interfaces*, 2019, **11**, 9804–9813.

166 D. Zhang, Z. Lin, S. Lan, H. Sun, Y. Zeng and X. Liu, *Mater. Chem. Front.*, 2019, **3**, 656–663.

167 D. Zhang, A. Zheng, J. Li, M. Wu, Z. Cai, L. Wu, Z. Wei, H. Yang, X. Liu and J. Liu, *Adv. Sci.*, 2017, **4**, 1600460.

168 H. Guo, T. Zhang, Y. Yu and F. Xu, *Trends Cell Biol.*, 2021, **31**, 520–524.

169 A. Dart, *Nat. Rev. Cancer*, 2018, **18**, 667.

170 T. K. Kim, E. N. Vandsemb, R. S. Herbst and L. Chen, *Nat. Rev. Drug Discovery*, 2022, **21**, 529–540.

171 T. Souho, L. Lamboni, L. Xiao and G. Yang, *Biotechnol. Adv.*, 2018, **36**, 1928–1945.

172 J. D. Martin, H. Cabral, T. Stylianopoulos and R. K. Jain, *Nat. Rev. Clin Oncol.*, 2020, **17**, 251–266.

173 M. Chakraborty, K. Chu, A. Shrestha, X. S. Revelo, X. Zhang, M. J. Gold, S. Khan, M. Lee, C. Huang, M. Akbari, F. Barrow, Y. T. Chan, H. Lei, N. K. Kotoulas, J. Jovel, C. Pastrello, M. Kotlyar, C. Goh, E. Michelakis, X. Clemente-Casares, P. S. Ohashi, E. G. Engleman, S. Winer, I. Jurisica, S. Tsai and D. A. Winer, *Cell Rep.*, 2021, **34**, 108609.

174 J. Galon and D. Bruni, *Nat. Rev. Drug Discovery*, 2019, **18**, 197–218.

175 M. Panagi, F. Mpekris, P. Chen, C. Voutouri, Y. Nakagawa, J. D. Martin, T. Hiroi, H. Hashimoto, P. Demetriou, C. Pierides, R. Samuel, A. Stylianou, C. Michael, S. Fukushima, P. Georgiou, P. Papageorgis, P. C. Papaphilippou, L. Koumas, P. Costeas, G. Ishii, M. Kojima, K. Kataoka, H. Cabral and T. Stylianopoulos, *Nat. Commun.*, 2022, **13**, 7165.

176 A. Stylianou, F. Mpekris, C. Voutouri, A. Papoui, A. Constantinidou, E. Kitiris, M. Kailides and T. Stylianopoulos, *Acta Biomater.*, 2022, **154**, 324–334.

177 Key reference: Z. Wei, X. Zhang, T. Yong, N. Bie, G. Zhan, X. Li, Q. Liang, J. Li, J. Yu, G. Huang, Y. Yan, Z. Zhang, B. Zhang, L. Gan, B. Huang and X. Yang, *Nat. Commun.*, 2021, **12**, 440.

178 J. Liu, Y. Tan, H. Zhang, Y. Zhang, P. Xu, J. Chen, Y. C. Poh, K. Tang, N. Wang and B. Huang, *Nat. Mater.*, 2012, **11**, 734–741.

179 V. Gensbittel, M. Krater, S. Harlepp, I. Busnelli, J. Guck and J. G. Goetz, *Dev. Cell*, 2021, **56**, 164–179.

180 J. H. Kim, A. F. Pegoraro, A. Das, S. A. Koehler, S. A. Ujwary, B. Lan, J. A. Mitchel, L. Atia, S. He, K. Wang, D. Bi, M. H. Zaman, J. A. Park, J. P. Butler, K. H. Lee, J. R. Starr and J. J. Fredberg, *Biochem. Biophys. Res. Commun.*, 2020, **521**, 706–715.

181 Key reference: X. Li, T. Yong, Z. Wei, N. Bie, X. Zhang, G. Zhan, J. Li, J. Qin, J. Yu, B. Zhang, L. Gan and X. Yang, *Nat. Commun.*, 2022, **13**, 2794.

182 M. Guo, F. Wu, G. Hu, L. Chen, J. Xu, P. Xu, X. Wang, Y. Li, S. Liu, S. Zhang, Q. Huang, J. Fan, Z. Lv, M. Zhou, L. Duan, T. Liao, G. Yang, K. Tang, B. Liu, X. Liao, X. Tao and Y. Jin, *Sci. Transl. Med.*, 2019, **11**, eaat5690.

183 Y. Gao, H. Zhang, N. Zhou, P. Xu, J. Wang, Y. Gao, X. Jin, X. Liang, J. Lv, Y. Zhang, K. Tang, J. Ma, H. Zhang, J. Xie, F. Yao, W. Tong, Y. Liu, X. Wang and B. Huang, *Nat. Biomed. Eng.*, 2020, **4**, 743–753.

184 H. Wang, H. Hu, H. Yang and Z. Li, *RSC Adv.*, 2021, **11**, 3226–3240.

185 E. Mohagheghian, J. Luo, J. Chen, G. Chaudhary, J. Chen, J. Sun, R. H. Ewoldt and N. Wang, *Nat. Commun.*, 2018, **9**, 1878.

186 W. Lee, N. Kalashnikov, S. Mok, R. Halaoui, E. Kuzmin, A. J. Putnam, S. Takayama, M. Park, L. McCaffrey, R. Zhao, R. L. Leask and C. Moraes, *Nat. Commun.*, 2019, **10**, 144.

187 S. Mok, S. Al Habyan, C. Ledoux, W. Lee, K. N. MacDonald, L. McCaffrey and C. Moraes, *Nat. Commun.*, 2020, **11**, 4757.

188 X. Ding, M. Li, B. Cheng, Z. Wei, Y. Dong and F. Xu, *Acta Biomater.*, 2022, **141**, 1–13.

189 E. Mohagheghian, J. Luo, F. M. Yavitt, F. Wei, P. Bhala, K. Amar, F. Rashid, Y. Wang, X. Liu, C. Ji, J. Chen, D. P. Arnold, Z. Liu, K. S. Anseth and N. Wang, *Sci. Rob.*, 2023, **8**, eadc9800.